2   **Flux variability of phyto- and zooplankton communities**

in the Mauritanian coastal upwelling between 2003 and 2008

Oscar E. Romero[1], Karl-Heinz Baumann[1,2], Karin A. F. Zonneveld[1], Barbara Donner[1], Jens Hefter[3],

6 *Bambaye Hamady[4], Vera Pospelova[5,6] and Gerhard Fischer[1,2]*

8   [1]University of Bremen, Marum, Center for Marine Environmental Sciences, Leobener Str. 8, 28359

Bremen, Germany.

10   [2]University of Bremen, Department of Geosciences, Klagenfurter Str. 2-4, 28359 Bremen,

Germany.

12   [3]Alfred Wegener Institute, Helmholtz Centre for Polar and Marine Research, 27568 Bremerhaven,

Germany.

14   [4]IMROP, Institut Mauretanien de Recherches Océanographiques et des Pêches, BP 22,

Nouadhibou, Mauritania.

16   [5]Department of Earth and Environmental Sciences, University of Minnesota, College of Science

and Engineering, 116 Church Street SE, Minneapolis, MN 55455, USA.

18   [6]School of Earth and Ocean Sciences, University of Victoria, OEASB A405, P. O. Box 1700 16

STN CSC, Victoria, British Columbia, V8W 2Y2, Canada.

22   **Keywords:** Eastern Boundary Upwelling Ecosystems, fluxes of microorganisms, interannual

variability, northwest Africa, primary producers, secondary producers, sediment traps

Abstract

26   Continuous multiyear records of sediment trap-gained microorganism fluxes are scarce. Such

studies are important to identify and to understand the main forcings behind seasonal and

28 multiannual evolution of microorganism flux dynamics. Here, we assess the long-term flux

variations and population dynamics of diatoms, coccolithophores, calcareous and organic

30   dinoflagellate cysts, foraminifera and pteropods in the Eastern Boundary Upwelling Ecosystem of

the Canary Current. A multiannual, continuous sediment trap experiment was conducted at the

32   mooring site CB_{eu} (*Cape Blanc eutrophic*, ~20°N, 18°W; trap depth = ca. 1,300 m) off Mauritania

(northwest Africa), between June 2003 and March 2008. Throughout the study, the reasonably

34   consistent good match of fluxes of microorganisms and bulk mass reflects the seasonal

occurrence of the main upwelling season and relaxation, and the contribution of microorganisms to

36   mass flux off Mauritania. A clear successional pattern of microorganisms, *i.e.* primary producers

followed by secondary producers, is not observed. High fluxes of diatoms, coccolithophores,

38   organic dinoflagellate cysts, and planktonic foraminifera occur simultaneously. Peaks of calcareous

dinoflagellate cysts and pteropods mostly occurred during intervals of upwelling relaxation. A

40   striking feature of the temporal variability of populations' occurrence is the persistent pattern of

seasonal groups' contribution. Species of planktonic foraminifera, diatoms, and organic

42   dinoflagellate cysts typical of coastal upwelling as well as cooler water planktonic foraminifera and

the coccolithophore *Gephyrocapsa oceanica* are abundant at times of intense upwelling (late

44   winter through early summer). Planktonic foraminifera and calcareous dinoflagellate cysts are

dominant in warm pelagic surface waters and all pteropod taxa are more abundant in fall and

46   winter, when the water column stratifies. Similarly, coccolithophores of the upper- and lower photic

zone, together with *Emiliania huxleyi,* and organic dinoflagellate cysts dominate the assemblage

48   during phases of upwelling relaxation and deeper layer mixing.

     A significant shift in the 'regular''' seasonal pattern of taxa relative contribution is observed

50   between 2004 and 2006. Benthic diatoms strongly increased after fall 2005 and dominated the

diatom assemblage during main upwelling season. Additional evidence for a change in population

52   dynamics are the short dominance of the coccolithophore *Umbilicosphaera annulus,* the

occurrence of the pteropod *Limacina bulimoides,* and the strong increase in the flux of calcareous

54   dinoflagellate cysts, abundant in tropical, warm oligotrophic waters south of the study area after fall

2005. Altogether, this suggests that pulses of southern waters were transported to the sampling

56   site via the northward Mauritania Current. Our multiannual trap experiment provides a unique

opportunity to characterize temporal patterns of variability that can be extrapolated to other

58   EBUEs, which are experiencing or might experience similar future changes in their plankton

community.

60

1. Introduction

62   A way to obtain insights into the impact of climate variability on marine ecosystems is

monitoring multiannual evolution and changes covering key species or groups of species

64   representing different trophic levels. To date, multiyear continuous, *in situ* monitoring records of

marine communities are scarce. Information about open ocean ecosystems is even more rare

66   (*e.g.*, IOC-UNESCO TS129 IGMETS 2017; Bringué et al., 2019). Furthermore, records providing

information about organism groups of different trophic levels are practically unknown or cover only

68   a few species (*e.g.*, Schlüter et al., 2012; Rembauville et al., 2016).

Eastern Boundary Upwelling Ecosystems (EBUEs) are among the most important marine

70   ecosystems, both ecologically and economically (Cropper et al., 2014). Despite the fact that they

cover only 10% of the global surface ocean area, they provide about 25% of the global fish catch

72   (Pauly and Christensen, 1995) and build extraordinary marine hotspots of high primary production

and biodiversity (Arístegui et al., 2009). In doing so, they play a key role in the marine biological

74   pump, as together with other continental margins may be responsible for more than 40% of the

CO_2 ocean sequestration (Muller-Karger et al., 2005). As EBUEs are highly dynamic with large

76   seasonal and interannual variability (*e.g.*, Chavez and Messié, 2009; Fischer et al., 2016), gaining

information on their long-term variability is essential to understand their potential response to

78   current global climate change.

One of the EBUEs that have been thoroughly studied over the past three decades is the coastal

80   ecosystem off Mauritania (northwest Africa), which is part of the Canary Current (CC) EBUE

(Cropper et al., 2014). The Mauritanian system is characterized by intense offshore Ekman

82   transport and strong mesoscale heterogeneity, which facilitate the exchange of neritic and pelagic

water masses (Mittelstaedt, 1983; Zenk et al., 1991; Van Camp et al., 1991; Arístegui et al., 2009;

84   Chavez and Messié, 2009; Meunier et al., 2012; Cropper et al., 2014). In addition, regional factors

such as nutrient trapping efficiency (Arístegui et al., 2009), the giant chlorophyll filament (Gabric et

86   al., 1993; Barton, 1998; Lange et al., 1998; Helmke et al., 2005); dust deposition (Fischer et al.,

2016, 2019) and/or the shelf width (Hagen, 2001; Cropper et al., 2014) strongly affect the temporal

88   dynamics of primary and secondary producers communities in surface waters along the

Mauritanian coast. In this ecosystem, several long-term, continuous, sediment trap-based

90   monitoring records are available since the late 1980s. Until now, studies monitoring variability of

this seasonally dynamic ecosystem mostly focused on the variability of bulk fluxes (Fischer et al.,

92   1996, 2009, 2016, 2019; Bory et al., 2001; Marcello et al., 2011; Skonieczy et al., 2013), particular

groups of microorganisms (Lange et al. 1998; Romero et al., 1999, 2002, 2003; Köbrich and

94   Baumann, 2008; Romero and Armand, 2010; Zonneveld et al., 2010; Köbrich et al., 2016; Romero

and Fischer, 2017; Guerreiro et al., 2019) or sea-surface temperature (Müller and Fischer, 2001;

96   Mollenhauer et al., 2015). However, the simultaneous comparison of the seasonal and interannual

dynamics of several phyto- and zooplankton communities by means of multiyear sediment trap

98   experiments has not been performed in this region and is rare in other EBUEs or other ocean

areas as well (Bringué et al., 2019).

100   This paper builds on the long-term studies of the variability of sea-surface temperature and

fluxes (SST) at the site CBeu published by Mollenhauer et al. (2015), Romero and Fischer (2017),

102   and Fischer et al. (2019). We describe the seasonal and interannual variability of fluxes of several

primary and secondary producers in the Mauritanian coastal upwelling over a continuous trap

104   experiment extending almost 1,900 days between June 2003 and March 2008 (Table 1). In

addition to the previously reported diatom fluxes and reconstructed SST values, we present here

106   new data of fluxes of coccolithophores, calcareous and organic-walled dinoflagellate cysts,

planktonic foraminifera and pteropods as well as the species-specific composition of the

108   assemblages that have been collected at the mooring site CBeu (*Cape Blanc eutrophic*), located

around 80 nm west of the Mauritanian coastline below a giant chlorophyll filament (Fig. 1). The

110   microorganisms producing the calcareous, opaline or organic remains have different water column

habitats, life strategies, and use different nutrient sources (Romero et al., 1999, 2002; Baumann et

112   al., 2005; Romero and Armand, 2010; Zonneveld et al., 2013), and are widely used as proxies in

paleostudies carried on Mauritanian sediments (Jordan et al., 1996; Romero et al., 2008; McKay et

114   al., 2014) and similar paleoenvironments (*e.g.*, Baumann and Freitag, 2004; Bouimetarhan et al.,

2009; Romero et al., 2015; Weiser et al., 2016; Hardy et al., 2018). The emphasis of our

116   multiannual trap experiment is on the comparison of temporal dynamics and the species-specific

composition of the primary and secondary producer plankton community off Mauritania. The

118   simultaneous assessment of fluxes of several microorganism groups collected over long intervals

provides substantial information about potential changes in the coastal upwelling community.

120   Results are discussed in the context of varying environmental conditions of the low-latitude

Northeastern Atlantic. To our knowledge, this is the first multiyear trap-based record of major

122   primary and secondary producers that provides multiyear information on the dynamics of major

components of the plankton community in a highly productive EBUE.

124   **2. Oceanographic setting of the study area**

The CC-EBUE is located in the eastern part of the North Atlantic Subtropical Gyre (Fig. 1;

126   Arístegui et al., 2009; Chavez and Messié, 2009; Cropper et al., 2014). Both the temporal

occurrence and the intensity of the upwelling along northwestern Africa depend on the shelf width,

128   the seafloor topography, and wind direction and strength (Mittelstaedt, 1983; Hagen, 2001). The

Mauritanian shelf is wider than the shelf northward and southward and gently slopes from the

130   coastline into water depths below 200 m (Fig. 1b; Hagen, 2001). The shelf break zone with its

steep continental slope extends over a distance of approximately 100 km (Hagen, 2001). As a

132   result of the coastal and shelf and slope topography, the ocean currents and wind systems, the

coastal region off Mauritania is characterized by almost permanent upwelling. Its intensity varies

134   throughout the year (Lathuilière et al., 2008; Cropper et al., 2014). Our trap site CBeu is located at

the southern boundary of this permanent upwelling zone (Fig. 1; Table 1).

136   The surface hydrography is strongly influenced by two wind-driven surface currents: the

southwestward-flowing CC and the poleward-flowing coastal countercurrent or Mauritania Current

138   (MC) (Fig. 1). The eastern branch of the subtropical gyre, the surficial CC detaches from the

continental slope between 25° and 21°N and supplies waters to the North Equatorial Current. The

140   CC water is relatively cool because it entrains upwelled water from the coast as it moves

southward (Mittelstaedt, 1991). The MC gradually flows northward along the coast up to about

142   20°N (Mittelstaedt, 1991), bringing warmer surface waters from the equatorial realm into the study

area. Towards late autumn, the MC is gradually replaced by a southward flow associated with

144   upwelling water due to the increasing influence of trade winds south of 20°N (Zenk et al., 1991),

and becomes a narrow strip of less than 100 km width in winter (Mittelstaedt, 1983). The MC

146 advances onto the shelf during summer and is enhanced by the relatively strong Equatorial

Countercurrent and the southerly monsoon (Mittelstaedt, 1983). The presence of strong coastal

148 currents during the upwelling season causes substantial horizontal shear within the surface layer,

where currents tend to converge (Mittelstaedt, 1983). This convergence favors the formation of the

150 Cape Verde Frontal Zone (CVFZ, Fig. 1; Zenk et al., 1991).

A coastal countercurrent, the Poleward Undercurrent (PUC; Fig. 1) occurs mainly due to wind-

152 driven offshore divergence (Pelegrí et al., 2017). North of Cape Blanc (ca. 21°N), the intense

northeasterly winds cause the coastal upwelling to move further offshore and the upper slope is

154 filled with upwelled waters. South of Cape Blanc, northerly winds dominate throughout a year, but

surface waters remain stratified and the PUC occurs as a subsurface current. South of Cape

156 Timiris (ca. 19°30'N), the PUC intensifies during summer-fall and remains at the subsurface during

winter–spring (Pelegrí et al., 2017). The encountering of the northward flowing MC-PUC system

158 with the southward flowing currents in the Canary Basin leads to flow confluence at the CVFZ

(Zenk et al., 1991) and the offshore water export visible as the giant Mauritanian chlorophyll

160 filament (Gabric, 1993; Pelegrí et al., 2006; Pelegrí et al., 2017). This filament extends over 300

km offshore (*e.g.*, Van Camp et al., 1991; Arístegui et al., 2009; Cropper et al., 2014) and carries

162 South Atlantic Central Water (SACW) offshore through an intense jet-like flow (Meunier et al.,

2012; Fig. 1). Intense offshore transport forms an important mechanism for the export of cool,

164 nutrient-rich shelf and upper slope waters offshore Mauritania. Based on satellite imagery and *in*

situ data, it has been estimated that the giant Mauritanian filament could export about 50% of the

166 particulate coastal new production offshore toward the open ocean during intervals of most intense

upwelling, while coastal phytoplankton at the surface might be transported as far as 400 km

168 offshore (Gabric et al., 1993; Barton, 1998; Lange et al., 1998; Helmke et al., 2005). The transport

effect could extend to even more distant regions in the deep ocean, since sinking particles are

170 strongly advected by lateral transport (Fischer and Karakaș, 2009; Karakaș et al., 2006; Fischer et

al., 2009).

172 The nutrient concentration of the upwelled waters off Mauritania varies depending on their origin

(Fütterer, 1983; Mittelstaedt, 1991; Zenk et al., 1991). The source of upwelling waters off

174 Mauritania are either North Atlantic Central Water (NACW), north of about 23°N, or SACW (south

of 21°N, Fig. 1). Both water masses are mixed in the filament area off Cape Blanc. The SACW

176   occurs in layers between 100 and 400 m depth off Cape Blanc and the Banc d'Arguin. The

hydrographic properties of the upwelling waters on the shelf suggest that they ascend from depths

178   between 100 and 200 m south off the Banc d'Arguin (Mittelstaedt, 1983). North of it, the SACW

merges gradually into deeper layers (200-400 m) below the CC (Mittelstaedt, 1983). During intense

180   upwelling, the stratification of the shelf waters weakens, and so is the stratification further offshore,

usually within the upper 100 m (Mittelstaedt, 1991). The biological response is drastically

182   accelerated in the upwelling waters when the SACW of the upper part of the undercurrent feeds

the onshore transport of intermediate layers to form mixed-water types on the shelf (Zenk et al.,

184   1991).

3. Material and Methods

186

3.1. Moorings, sediment traps and bulk flux assessment

188   Sediment trap moorings were deployed at site CBeu off Mauritania in the CC-EBUE (Fig. 1).

Details on trap location and depth, sample amount, water depth and sampling intervals as well as

190   the sample identification (cruise and GeoB numbers) are presented in Table 1. Large-aperture

time-series sediment traps of the Kiel type were used with 20 to 40 cups (depending on ship-time

192   availability) and 0.5 m² openings, equipped with a honeycomb baffle (Kremling et al., 1996). Traps

were moored in intermediate waters (1,256 m – 1,296 m) and sampling intervals varied between

194   6.5 and 23 days (Table 1). Uncertainties with the trapping efficiency due to strong currents (*e.g.*

undersampling) and/or due to the migration and activity of zooplankton migrators ('swimmer

196   problem') are assumed to be minimal in the depth range of our trap experiments (Buesseler et al.,

2007; Fischer et al., 2019).

198   Prior to each deployment, sampling cups were poisoned with 1 ml of concentrated $HgCL_2$ per

100 ml of filtered seawater. Pure NaCl was used to increase the density in the sampling cups up to

200   40 ‰. Upon recovery, samples were stored at 4°C and wet split in the MARUM sediment trap

laboratory (University Bremen, Bremen) using a rotating McLANE wet splitter system. Larger

202   swimmers, such as crustaceans, were handpicked with forceps and removed by carefully filtering

through a 1-mm sieve. All flux data hereafter refer to the size fraction of <1 mm. Detailed

204 information about sampling and laboratory analysis is given in Mollenhauer et al. (2015), Romero

and Fischer (2017) and Fischer et al. (2019). These papers present the bulk fluxes for the

206 deployments CBeu 1-5 (Table 1). Alkenone-derived sea surface temperature (SST) for the CBeu

deployments 1-4 were provided by Mollenhauer et al. (2015).

208   Using ¼ or $^1/_5$ wet splits, analysis of the <1 mm fraction was carried out (Fischer and Wefer,

1991; Fischer et al., 2016). Samples were freeze-dried and homogenized before being analyzed

210 for bulk (total mass), organic carbon (OC), calcium carbonate ($CaCO_3$) and biogenic silica (BSi,

opal). Total organic carbon (TOC) and $CaCO_3$ were measured by combustion with a CHN-Analyzer

212 (HERAEUS, Department of Geosciences, University of Bremen). TOC was measured after

removal of carbonate with 2 N HCl. Overall analytical precision based on internal lab standards

214 was better than 0.1% (±1σ). Carbonate was determined by subtracting OC from total carbon, the

latter being measured by combustion without pre-treatment with 2N HCl. Organic matter was

216 estimated by multiplying the content of total organic carbon by a factor of two as about 50-60% of

marine organic matter is constituted by OC (Hedges et al., 2002).

218   BSi was determined with a sequential leaching technique with 1M NaOH at 85°C (Müller and

Schneider, 1993). The precision of the overall method based on replicate analyses is mostly

220 between ±0.2 and ±0.4%, depending on the material analyzed. The lithogenic fluxes were

estimated by subtracting the masses of $CaCO_3$, BSi, and 2 x OC from the total mass flux.

222 **3.2. Assessment of organism fluxes and species identification**

3.2.1. Diatoms

224   Diatom data shown here were previous published in Romero and Fischer (2017). For this study

1/25 and 1/125 splits of the original samples were used. Samples were prepared for diatom studies

226 following the method proposed by Schrader and Gersonde (1978). A total of 185 sediment trap

samples were processed. Each split was treated with potassium permanganate, hydrogen

228 peroxide, and concentrated hydrochloric acid following previously used methodology (Romero et

al., 2002, 2009a, b, 2016, 2017). Identification and count of the species assemblage were done on

230 permanent slides (*Mountex*® mounting medium) at x1000 magnification using a *Zeiss*®Axioscop

with phase-contrast illumination (MARUM, Bremen). The counting procedure and definition of

232 counting units follows Schrader and Gersonde (1978). Depending on valve abundances in each

sample, several traverses across each slide were examined. Total amount of counted valves per

234   slide ranged between 300 and 800. At least two cover slips per sample were scanned in this way.

Valve counts of replicate slides indicate that the analytical error of concentration estimates is ca.

236   10 %. The resulting counts yielded abundance of individual diatom taxa (absolute and relative) as

well as daily fluxes of diatoms as valves per m^{-2} d^{-1}, calculated according to Sancetta and Calvert

238   (1988).

3.2.2. Coccolithophores

240   Aliquots of each sample were 1/125. Depending on the total flux, samples were further split

down to 1/625 to 1/2500 of the original sample volume and were filtered afterward onto

242   polycarbonate membrane filters (Schleicher and Schuell^{TM} 47mm diameter, 0.45 µm pore size). A

piece of the filter was cut and mounted on a Scanning Electron Microscopy stub. Qualitative and

244   quantitative analyses of the trapped assemblages were performed using a *Zeiss*® DSM 940A at

10kV accelerating voltage (Department of Geosciences, University of Bremen, Bremen). In an

246   arbitrarily chosen transect, coccoliths were counted until a total of at least 500 specimens were

reached. The taxonomic classification of identified species was based on Young et al. (2003) as

248   well as on Nannotax 3 (Young et al., 2019).

3.2.3. Calcareous and organic-walled dinoflagellate cysts

250   1/125 splits of the original trap material were ultrasonically treated and sieved with tap water

through a high precision metal sieve (Storck-Veco®) with a 20 µm pore size. The residue was

252   transferred to Eppendorff cups and concentrated to 1 ml of suspension. After homogenization of

the material, a known aliquot was transferred to a microscope slide where it was embedded in

254   glycerin-gelatine, covered with a cover slip and sealed with wax to prevent oxidation of the

organic material. After counting, cyst fluxes were calculated by multiplying the cyst counts with

256   the aliquot fraction and the split size (1/125) and dividing through the amount of days during

which the trap material was sampled as well as the trap-capture surface. No chemicals were

258   used to prevent dissolution of calcite and silicate. Cyst assemblages were determined by light

microscopy (Axiovert, x400 magnification). The taxonomy of calcareous dinoflagellate cysts

260   follows Vink et al. (2002) and Elbrächter et al. (2008), while that of organic walled dinoflagellate

cysts is according to Zonneveld and Pospelova (2015),

262 **3.2.4. Planktonic foraminifera and pteropods**

Depending on the absolute magnitude of the total mass flux, a 1/5 or a 1/25 split of the wet

264 solution (fraction <1mm) was used to pick planktonic foraminifera and pteropods (pelagic

mollusks). Specimens of both groups of calcareous microorganisms were rinsed three times by

266 using tap water, dried at 50°C in an oven overnight and then separated from each other.

Identification and count of shells were done by using a stereomicroscope *Zeiss*® Stemi 2000

268 (MARUM, Bremen). The foraminifera fluxes (all size fractions) were determined in mg per m^2 and

day with a Sartorius BP 211D analytical balance. Additionally, the total amount of

270 specimens/sample of foraminifera and pteropods (>150 μm) were manually counted. Planktonic

foraminifera were identified and classified according to Hemleben et al. (1989) and Schiebel and

272 Hemleben (2017). Out of 15 species of planktonic foraminifera identified, only six species were

used as environmental indicators.

274 **3.2.5. Alkenones**

1/5 wet splits of the <1 mm fraction were used for alkenone analysis. Briefly, freeze-dried CBeu

276 1-4 samples were solvent extracted. The resulting total lipid extracts (TLEs) saponified and the

alkenone fractions were obtained by means of column chromatography of the neutral lipid fractions

278 from the saponification. Details are given in Mollenhauer et al. (2015).

A slightly different, miniaturized analysis procedure has been applied for the CBeu trap 5

280 samples. 1/5 wet splits of the freeze-dried <1mm fraction were weighted in 10 ml Pyrex tubes and

a known amount of an internal standard (*n*-Nonadecan-2-one) was added. Samples were then 3x

282 ultrasonically extracted with a mixture of 3 ml dichloromethane/methanol (9:1 vol./vol.), centrifuged

and the supernatant solvent combined as total lipid extract (TLE). TLEs were evaporated to

284 dryness and saponified in a 0.1M potassium hydroxide solution in methanol/water (9:1 vol./vol.) for

two hours at 80°C. Neutral lipids, recovered with hexane, were afterwards separated into fractions

286 of different polarity by silica gel chromatography and elution with hexane, dichloromethane/hexane

(1:1 vol./vol.) and dichloromethane/methanol (9:1 vol./vol.), respectively. The second fraction

288 containing the alkenones was dried, re-dissolved in 20μl hexane and analyzed on a 7890A gas

chromatograph (GC, Agilent Technologies) equipped with a cold on-column injection system, a

290 DB-5MS fused silica capillary column (60 m, ID 250 μm, 0.25 μm film coupled to a 5 m, ID 530 μm

deactivated fused silica precolumn) and a flame ionization detector (FID). Helium was used as carrier gas (constant flow, 1.5 mL/min) and the GC oven was heated using the following temperature program: 60°C for 1 min, 20°C/min to 150°C, 6°C/min to 320°C and a final hold time of 35 min. Alkenones were identified by comparison of the retention times with a reference sample composed of known compounds. Peak areas were determined by integrating the respective peaks.

The $U_{37}^{K'}$ index was calculated using the following equation (Prahl and Wakeham, 1987)

$$U_{37}^{K'} = \frac{C_{37:2}}{C_{37:2}+C_{37:3}}$$

and converted to SST using the global surface water calibration from Conte et al. (2006):

$$SST = \frac{U_{37}^{K'} - 0.0709}{0.0322}$$

3.3. Environmental physical parameters

SST, Sea Surface Temperature Anomaly (SSTA), mixed layer depth (MLD) and upper ocean chlorophyll-a concentration data are based on satellite-derived data achieved from the NASA supported Giovanni project (https://giovanni.gsfc.nasa.gov/). SST is the mean of daily surface ocean temperature and MLD values of the sampling interval in a 4 km^2 area around the trap position (Table 1). In the study area, SST at the mooring location is influenced by seasonal air temperature changes as well as the presence of upheld water surfacing at the trap position.

To compensate for seasonal air temperature changes the SSTA is calculated by subtracting the above-calculated SST at the trap position from mean SST values of simultaneous sampling intervals in a 4 km^2 block 200 nm west of the trap position. Both SSTA and MLD are parameters reflecting active upwelling in the study area. Upper ocean chlorophyll a data and MLD represent monthly mean values in a 9 km^2 block around the trap position. Wind speed and wind directions are provided by Nouadhibou airport (20°56′N, 17°2′W) (Institut Mauretanien de Recherches Océanographiques et des Pêches, Nouadhibou, Mauritania). For statistical analyses, the means of daily values during the trap sampling intervals were calculated.

3.4. Multivariate analyses

To determine if a linear or unimodal based ordination method should be applied on the data we performed a Detrended Correspondence Analysis previous to the statistical analysis. Results of

318 this analysis revealed a total length of gradient of 1.2 sd, which indicates a linear species respond

on environmental gradients. The ordination techniques Principal Component (PCA) and

320 Redundancy Analysis (RDA) have been accordingly performed. Significance of the environmental

variables has been tested with a Monte-Carlo permutation test with unrestricted permutations.

322   PCA and RDA have been performed with the software Package Canoco 5 (ter Braak and

Smilauer, 2012; Smilauer and Leps, 2014). To obtain insights into the temporal relationship

324 between fluxes of organism groups (diatoms, coccolithophores, calcareous and organic-walled

dinoflagellate cysts, planktonic foraminifera and pteropods) and bulk components as well as the

326 environmental conditions in surface waters and low atmosphere, a RDA has been performed. RDA

compares the total flux of organism groups with environmental parameters and TOC, BSi, $CaCO_3$

328 and lithogenic fluxes (Table 2). Since the fluxes of the individual groups differ by several orders of

magnitudes, it is essential to normalize their flux values prior to the statistical analysis in order to

330 be able to determine temporal relationships of flux variability. As a consequence, the total flux of

the organism groups has been normalized to values between 0 and 1000 previous to the analyses

332 according to formula 1:

$nFl_i = (FL_{i/y}/ FL_i max) \times 1000n$

334   Fl_i = normalized flux of species group i

$Fl_{i/y}$ = flux of species group i in sample y

336        $FL_i max$ = maximal flux observed in species group i

To better understand the relationship within the individual organism groups, a PCA has been

338 performed (Table 2). For these analyses, the total flux of the organisms/species groups have been

normalized to values between 0 and 1000 according to formula 2:

340 $nFl_j = (FL_{ij/y}/ FL_i max) \times 1000n$

Fl_j = normalized accumulation rate of ecological entity j in species group i

342        $Flj_{/y}$ = accumulation rate of ecological entity j in sample yFL_j max = maximal accumulation

rate observed in species group i

344 Within coccolithophores, *Umbilicosphaera anulus* had exceptionally large fluxes in one sample

only. This flux exceeded the maximal flux of the other species by a factor of three. This value has

346 been excluded from the analysis and the FL_j max in this group is determined by excluding this

outlier.

348

4. Results

350   **4.1. Bulk fluxes and fluxes of organism groups**

Independent of the year, the total mass flux of particulates at site CBeu is mainly composed of

352   biogenic components (calcium carbonate, BSi and TOC, Table 3; Fischer et al., 2019). Calcium

carbonate is the main bulk biogenic component. The daily average flux of $CaCO_3$ –calculated for

354   each full calendar year sampled between 2004 and 2007- varies between 121.1 and 150.9 mg m^{-2}

d^{-1} (Table 3). BSi is the second most important biogenic bulk component (35.8-54.61 mg m^{-2} d^{-1},

356   Table 3), followed by TOC (19.00-29.40 mg m^{-2} d^{-1}). Lithogenics is the main non-biogenic

contributor to the total mass flux (84.6-134.2 mg m^{-2} d^{-1}, Table 3). Coccolithophores, planktonic

358   foraminifera, calcareous dinoflagellates and pteropods are main contributors to the $CaCO_3$ flux,

while diatoms dominate the siliceous community.

360   The fluxes of total mass, $CaCO_3$, TOC, BSi and lithogenics show major peaks in winter and

spring (Fig. 2). Secondary maxima were found during late summer/fall, mainly in 2003, and less

362   clearly in 2005, 2006 and 2007 (Fig. 2). However, the individual components reveal different flux

amplitudes and point to some interannual variability (Table 3). $CaCO_3$ fluxes were exceptionally

364   high in early winter 2005 compared to the other years. Fluxes of BSi and TOC match well the flux

pattern of total mass and show less interannual variability (Fig. 2c, d). The flux of the lithogenic

366   fraction has the highest amplitudes in spring 2006 and 2007 (Fig. 2e).

Fluxes of microorganisms are dominated by diatoms and coccoliths (Fig. 3a, b). These

368   exceeded the fluxes of organic- and calcareous walled dinoflagellate cysts, planktonic foraminifera

and pteropods by a factor of four to five. Highest coccolithophore and diatom fluxes reach 4.2 x 10^9

370   coccoliths m^{-2} d^{-1}, and 1.2 x 10^8 valves m^{-2} d^{-1}, respectively. Maximal fluxes of organic-walled

dinoflagellates reach up to 7.1 x 10^4 cysts m^{-2} d^{-1}, of planktonic foraminifera 0.9 x 10^4 shells m^{-2} d^{-}

372   ^{1}, and of pteropods 1.1 x 10^4 shells m^{-2} d^{-1}.

Each group of microorganisms shows large seasonal and interannual variability (Table 5).

374   Diatoms had their maximal flux in fall/winter 2005 and spring/summer 2006 (Fig. 3a).

Coccolithophores had their highest fluxes mostly in winter/spring throughout the sampling interval

376 and exceptionally in July/August 2003 and 2007 and in fall 2005. On the long-term, low

coccolithophore fluxes were observed fall and winter 2007/2008 (Fig. 3b). Calcareous

378 dinoflagellate cysts were practically absent until fall 2005 (Fig. 3c). After September 2005,

calcareous dinoflagellate cysts showed maximal export fluxes in fall/winter 2005/2006 and

380 fall/winter 2006/2007 (Fig. 3c). Fluxes decreased again after spring 2007. Organic-walled

dinoflagellate cysts had their highest export fluxes in summer 2003, spring/summer 2006 and

382 summer 2007 (Fig. 3d). Planktonic foraminifera showed maximal fluxes in summer 2003,

winter/spring 2004, 2005, 2007 and spring/summer 2006 (Fig. 3e). Pteropods had their maximal

384 fluxes in summer 2003, fall/winter 2003/2004, 2004/2005 and 2006/2007 as well as summer 2005

and 2007 (Fig. 3f).

386 **4.2. Species- and group-specific composition of assemblages**

The studied plankton community at the CBeu site is highly diverse and is composed by at least

388 220 identified species. Table 5 presents the species-specific composition of groups depicted in Fig.

4.

390 Out of 170 marine ***diatom*** species, the 70 most abundant diatom taxa (average relative

contribution >0.75% for the entire studied interval) were attributed to four groups, according to the

392 main ecological conditions they represent: (1) benthic, (2) coastal upwelling, (3) coastal planktonic,

and (4) open-ocean waters (see also Romero and Fischer, 2017). The diatom groups show a clear

394 seasonal pattern and strong interannual variability (Fig. 4a, Table 4). Benthic diatoms have higher

relative contributions during spring and summer, whereas the coastal upwelling group mainly

396 occurred between late spring and early fall. Open-ocean diatoms were more abundant from fall to

early spring while the coastal planktonic taxa tended to be more abundant during fall and winter.

398 Most noticeably, a drastic shift in the relative contribution of the benthic diatoms occurred in spring-

summer 2006 when the abundance of benthic diatoms strongly increased from 2006 onward,

400 compared to 2003–2005 (Fig. 4a, Table 4). In spite of the increased relative contribution of benthic

diatoms after 2005, the seasonal pattern of the predominantly high spring-summer total diatom flux

402 remained unaltered (Fig. 3a).

Coccolithophores are consistently dominated by *Emiliania huxleyi* and *Gephyrocapsa*

404 *oceanica*, whose combined contribution always represents > 50% of the community throughout the

406 sampling period (Fig. 4b, Table 4). Oligotrophic upper photic zone (UPZ, *e.g.*, *Umbellicosphaera tenuis*, *U. irregularis*) and lower photic zone species (LPZ, *e.g.*, *Florisphaera profunda*, *Gladiolithus flabellatus*) make up the majority of the remaining species. Whereas *E. huxleyi* showed a less clear

408 seasonal pattern, *G. oceanica* tends to be more abundant during late spring and early fall (Fig. 4b). In contrast, UPZ and LPZ taxa have higher relative contributions during winter and spring. The

410 appearance of *Umbilicosphaera anulus* (present in consistently low relative abundances of 5-10% until the summer of 2006) accounts for up to 65% of the community in winter 2005/06. Other

412 common taxa with an average relative contribution >0.75% for the entire studied interval are listed in Table 5.

414   ***Calcareous dinoflagellate cysts*** can be attributed to five groups based according to the main ecological conditions they represent (Siggelkow et al., 2002; Richter et al., 2007; Kohn and

416 Zonneveld, 2010); (1) upwelling, (2) warm waters, (3) terrestrial mineral input, (4) cosmopolitan and (5) other species (Table 5). Until fall 2005 abundances are very low such that the

418 recognition of a seasonal pattern is hampered (Fig. 4c). After fall 2005, their occurrence shows a clearer seasonal pattern. In spring-summer of 2006 upwelling species dominate the association.

420 After fall 2006, the community is composed by the interplay of cosmopolitan species, warm water taxa and upwelling-dependent species, where warm water taxa dominate. Whereas

422 upwelling species are most abundant in spring and fall, warm water and mineral indicators are more abundant in fall/winter (Fig. 4).

424   ***Organic dinoflagellate cysts*** can be attributed to five groups based on the relationship between their geographic distribution in surface sediments from the Cape Blanc area and the

426 environmental conditions in surface and subsurface waters as well as long-term surveys of their seasonal cyst production (Susek et al., 2005; Holzwarth et al., 2010; Smayda, 2010; Smayda

428 and Trainer, 2010; Trainer et al., 2010; Zonneveld et al., 2012, 2013): (1) upwelling, (2) upwelling relaxation, (3) potential toxic, (4) cosmopolitan, and (5) other species. Throughout the

430 investigated time interval upwelling species are abundant in spring and fall/winter whereas upwelling relaxation species have higher relative abundances in fall (Fig. 4d). Potential toxic

432 species are abundant in fall/winter 2004/2005 and 2007/2008. Organic-walled dinoflagellate

cysts do not show a clear change in their composition between 2005 and early 2006 (Table 4)

434   as observed for many other groups.

The distribution and abundance of **planktonic foraminifera** species is linked to surface-water

436   properties. We use prominent species as tracers of surface water properties: *Globigerina bulloides*,

usually thriving in temperate to subpolar waters during intervals of enhanced primary productivity

438   due to high nutrient availability (Schiebel and Hemleben, 2017), is generally most abundant

between summer and fall (fig. 4e). Transitional and subpolar species *Globorotalia inflata* and

440   *Neogloboquadrina incompta* are usually present throughout a year, only decreasing in abundance

in fall and winter when warm water taxa peaked (*Globigerinoides ruber* pink, *G. ruber* white and *G.*

442   *sacculifer*; Kucera, 2007, Schiebel and Hemleben, 2017) (Fig. 4e). The only exception is in fall and

winter 2004/2005, when warm-water taxa are almost absent.

444   As large secondary carbonate producers off Mauritania, **pteropods** are important contributors

to the carbonate flux in the CC-EBUE (Fischer et al., 2016). The community is composed of

446   relatively few taxa. *Heliconoides inflatus* dominates the assemblage throughout most of the studied

interval (Fig. 4f). It is often the only species found in the assemblage until winter 2005/2006, when

448   a sudden and drastic shift in the relative contribution occurred. *Limacina bulimoides* appears for

the first time in winter to spring 2006 - and again in fall and winter 2006/2007 - and dominates the

450   assemblage together with a group of unspecified uncoiled pteropods. However, another

occurrence of *L. bulimoides* is missing in winter 2007/2008.

452   **4.3. Statistical analyses**

Comparison of the fluxes of the microorganisms, bulk components and the environmental

454   conditions in surface waters and the lower atmosphere (MLD, average wind speed, wind direction,

chlorophyll-*a* concentration (Chl-*a*), SST and SSTA) resulted in a significant relationship within the

456   first and second RDA axes that correspond to 34 % and 11% of the variance within the dataset,

respectively (Table 2).

458   All microorganism groups are ordinated on the positive part of the first axis showing a positive

relationship with all bulk parameters (Fig. 5). This implies that the fluxes of total mass, TOC, BSi

460   and $CaCO_3$ increased with increasing fluxes of all studied microorganism groups (Fig. 5, Tables 3

and 4). Fluxes of planktonic foraminifera, diatoms and –to a lesser extent– coccolithophores and

462 organic dinoflagellate cysts are ordinated on the negative site of SST and, with the exception of

organic dinoflagellate cysts, ordinated on the positive side of MLD (Fig. 5). This implies that their

464 fluxes are enhanced whenever SST is low and MLD is deep, *i.e.* under a well-mixed uppermost

water column. Diatoms, coccolithophores, organic dinoflagellate cysts and planktonic foraminifera

466 also show a positive correlation with SSTA, implying that enhanced fluxes of these microorganisms

occur when temperature anomalies between waters overlying site CBeu and the offshore pelagial

468 is large. The flux of pteropods and calcareous dinoflagellate cysts are positively related to the

average wind direction, and negatively to MLD and average wind speed (Fig. 5).

470  Interestingly, the satellite-derived Chl-a data do not show a significant correlation with fluxes of

major microorganism groups studied at site CBeu. This possibly indicates that (1) a large portion of

472 satellite-measured chlorophyll concentration is delivered by microorganisms, which did not reach

the CBeu trap, and/or (2) due to the strong ballasting effect, part of the microorganisms' remains

474 reach the trap cups independent of intervals of highest satellite chlorophyll values. An alternative

explanation is that (3) satellites measure the chlorophyll concentration in the uppermost

476 centimeters of the water column while microorganisms collected with the CBeu traps thrive mostly

in waters deeper than those reached by satellite sensors.

478  To better understand the correlation of the fluxes of the species groups within the

microorganism groups, PCA has been performed (Fig. 6, Table 2). The first two axes correspond

480 to 26.3 % and 16.2% of the variance within the dataset respectively. Based on their ordination on

the first and second axis, three groups are recognized (Fig. 6):

482  - Groups 1 and 2 are ordinated at the negative side of the second axis. Group 1 (in blue, Fig.

    6) is built by planktonic foraminifera characteristic of cooler or high nutrient water masses

484    (For-cold, For-hinut); benthic and upwelling-related diatoms (Dia-bent and Dia-upw);

    organic dinoflagellates characteristic for upwelling regions (OD-upw), and the

486    coccolithophore *Gephyrocapsa oceanica* (Co-*Gocean*). Group 2 (in brown, Fig. 6) consists

    of upwelling–related and other calcareous dinoflagellates cysts (CD-upw and CD-other),

488    other coccolithophores (Co-other), and coastal planktonic and open-ocean diatoms (Dia-

    coast and Dia-ocean).

490  - Ordinated on the positive side of the second axis and central part of the first axis, group 3

492   assembles planktonic foraminifera mainly thriving in warm waters (For-warm), calcareous dinoflagellates characteristic of warm water conditions and those responding to mineral input (CD-warm, CD-min), and all pteropods taxa (in black, Fig. 6).

494   - Group 4 is ordinated at the central/positive part of the second axis and positive site of the first axis. Species assigned to group 4 are: organic walled dinoflagellate cysts typical of the

496   upwelling relaxation (OD-upw relax); UPZ and LPZ coccolithophores (Co-up phot and Co-low phot); *E. huxleyi* (Co-*Ehux*), other coccolithophores (Co-other), *U. anulus* (Co-*Uanu*),

498   and cosmopolitan calcareous dinoflagellate cysts (CD-cosm) (in red, Fig. 6).

500 **5. Discussion**

5.1. Relationship between microorganisms' fluxes at site CBeu and the physical and

502 **biogeochemical settings off Mauritania**

Both the visual examination of the flux variability and the performed statistical analysis evidence

504 that the seasonality of most microorganism groups at the CBeu site closely follows the temporal pattern of changes in upper water oceanographic conditions off Mauritania between June 2003

506 and March 2008. Fluxes of diatoms, coccolithophores, organic-walled dinoflagellate cysts and planktonic foraminifera increase whenever the uppermost water column is well mixed (Fig. 7e),

508 SSTs are low (Fig. 7d), and SSTA are high (Figs. 2, 3, 5). This strong match supports the scenario of simultaneous occurrence of intense upwelling off Mauritania and high microorganisms' fluxes at

510 site CBeu. Several previous studies have separately documented enhanced production of diatoms, coccolithophores, organic-walled dinoflagellate cysts and planktonic foraminifera occurring when

512 the nutrient concentration in the uppermost water column off Mauritania increases (Baumann et al., 2005; Zonneveld et al., 2012; Guerreiro et al., 2017; Romero and Fischer, 2017; Pospelova et al.,

514 2018).

The atmospheric, hydrographic and biochemical conditions deliver the physical parameters and

516 nutrient conditions that determine the temporal pattern of population dynamics as recorded by the CBeu trap. Wind and upper water conditions off Mauritania show a clear seasonal pattern of

518 variability (Fig. 7a-e). The highly stratified uppermost water column (above 40 m water depth) overlying site CBeu is an effect of winds blowing mainly from the N-NE between late winter and

520   early summer (Fig. 7a, b, e). The stratification off Mauritania breaks down mostly in early to middle

winter, when the predominant winds turn from N-NE into S-SE (Fig. 7a). Following this setting,

522   upwelling reaches its highest intensity between late winter/early spring and early summer

(Mittelstaedt, 1991; Meunier et al., 2012; Cropper et al., 2014). The SST record (Fig. 7d) matches

524   well the seasonal alternation of stratification and mixing conditions: lowest temperatures occur

mostly between winter and early spring (increasing SSTA in late winter and throughout spring).

526   Throughout the period investigated, this SST cyclicity remains fairly constant.

        Fluxes of total mass and biogenic bulk components ($CaCO_3$, BSi, TOC) are clearly seasonal in

528   nature (Fig. 3 a-d; Fischer et al., 2019) and reflect the temporal productivity pattern of the

Mauritanian upwelling region (Meunier et al., 2012; Cropper et al., 2014). The good temporal

530   match between flux maxima of most of the studied microorganism groups and biogenic bulk

components unambiguously evidences the contribution of primary and secondary producers to the

532   total mass/biogenic mass fluxes off Mauritania (Figs. 2, 3). Higher absolute values of $CaCO_3$ over

BSi (Fig. 2b, d, Table 3) support the scenario of calcareous primary and secondary producers

534   (coccolithophores, planktonic foraminifera and pteropods) dominating the plankton community in

the Mauritanian upwelling system (Fischer et al., 2019). Diatoms are the main contributors to the

536   BSi flux (Fig. 3a, 2d; Romero et al., 2002; Romero and Fischer, 2017).

        A strong match among fluxes of diatoms, coccolithophores, organic-walled dinoflagellate cysts

538   and planktonic foraminifera with lithogenic fluxes at times of intense upwelling is observed (Figs.

2e, 3 a-c, e). The RDA supports this correlation (Fig. 5). The good correlation between lithogenic

540   and microorganisms' fluxes demonstrates that winds –responsible for the water column mixing off

Mauritania (Mittelstaedt, 1983; Meunier et al., 2012)– might additionally enrich surface waters

542   overlying site CBeu with land-derived nutrients. Primary and secondary producers may remarkably

benefit from this eolian-transported pool of nutrients. Lithogenic material is brought into

544   Mauritanian ocean waters in the form of dust that it is transported from the Sahara and the Sahel

(Romero et al., 2003; Friese et al., 2017). Numerous studies have thoroughly documented that the

546   particle flux off Mauritania predominantly occurs in the form of aggregates, often rich in lithogenic

particles (e.g., Karakaş et al., 2009; Iversen et al., 2010; Iversen and Ploug, 2010; Nowald et al.,

548   2015; Fischer et al., 2016; van der Jagt et al., 2018). Recent experiments have also shown that

550   aggregates' abundance and sinking velocities increase toward deeper waters when aggregates

are ballasted with lithogenic particles, whereas aggregates are not able to scavenge lithogenic

material from deeper waters (van der Jagt et al., 2018). Further evidence of a possible ballasting

552   effect on the flux of bulk components was recently presented by Fischer et al. (2019). These

authors observed that individual high BSi maxima at site CBeu revealed a peak-to-peak correlation

554   with the dust fluxes. This was interpreted to indicate a strong coupling between dust deposition

(lithogenic flux) and the efficiency of the biological pump under dry depositional conditions in winter

556   off Mauritania. Based on these observations, Fischer et al. (2019) proposed that the ballasted,

organic-rich aggregates built in surface waters immediately react to any additional dust supply with

558   aggregation followed by rapid sedimentation. Experimental studies on aggregate ballasting and

scavenging off Mauritania (van der Jagt et al., 2018) support this view as well.

560   A remarkable finding of our multiannual trap experiment is that flux maxima of diatoms,

coccolithophores, organic-walled cysts producing dinoflagellates (all primary producers) and

562   planktonic foraminifera (secondary producers) seem to occur fairly simultaneously (Figs. 3, 5). We

propose three possible interpretations: (*i*) no clear short-term succession of the microorganism

564   groups occurred (no temporal turnover in phytoplankton composition within a few days, Roelke and

Spatharis, 2015), (*ii*) the succession is not properly captured due to low temporal resolution of

566   some sediment trap intervals (Table 1), and/or (*iii*) the microorganisms –originally produced in

surface and subsurface waters by different communities– sink with different velocities through the

568   water column toward the ocean bottom and get 'mixed' during their sinking, mainly due to

dissimilar weights and sizes of their remains.

570   Although it is widely believed that the supply of resources regulates the marine community

structure (Roelke and Spatharis, 2015), experimental data show that the competition of resources

572   *per se* does not lead to succession of phytoplankton populations. For instance, Barber and Hiscock

(2006) observed that marine picoplankton is not replaced by diatoms when chemical transient

574   conditions (*e.g.*, added iron) abruptly provide a more favorable growth setting. The enormous

proportional increase in diatom biomass has fostered the misconception that diatoms replace the

576   non-diatom taxa by succession as the bloom matures. Additional evidence is provided by

observational studies. Bringué et al. (2018) observed that autotrophic dinoflagellates in the Cariaco

578 Basin do not appear to compete with diatoms for resources as both groups respond positively to

upwelling dynamics. Similarly, Anabalón et al. (2014) observed equal and simultaneous

580 contributions of diatoms and pigmented dinoflagellates to total autotrophic biomass off Cape Ghir

located in the northern CC-EBUEs. Contrary to conventional wisdom, Anabalón et al. (2014)

582 demonstrate that groups of phytoplankton increase in growth rates and absolute abundance, but

the biomass increase of the ambient non-diatom assemblage is modest, especially compared to

584 the order of magnitude or more increase of diatom biomass.

The first three CBeu trap experiments had long, low-resolution sampling intervals (>18

586 days/sample, June 2003 through September 2006, Table 1). However, the high-resolution intervals

of CBeu deployments 4 and 5 (up to 7.5 days per sample, Oct 2006-March 2008, Table 1) should

588 have captured a possible short-term succession of major groups (*e.g.*, diatoms quickly reacting to

increasing nutrient availability, whereas photosynthetic dinoflagellates becoming more abundant

590 during upwelling relaxation, Margalef, 1963; Jiménez-Quiroz et al., 2019). Although we do not

dismiss the possibly occurrence of succession within studied populations at site CBeu, at this

592 stage we do not disregard either its occurrence. It should also be kept in mind that the deployed

traps capture those microorganism remains that reach the trap cups at around 1,300 m water

594 depth, while they hardly capture green algae or cyanobacteria thriving in surface waters. CBeu

traps at ca. 1,300 m water depth capture a mixed signal of sinking particles from a surface

596 catchment area of at least ca. 100 km^2 (Siegel and Deuser, 1997, Fischer et al., 2016,) due to (*i*)

differential settling velocities of particles (Fischer and Karakaş, 2009; Iversen et al., 2010; van der

598 Jagt et al., 2018), and (*ii*) highly heterogeneous and dynamic surface water conditions due to

filament and eddy activity off Mauritania (Mittelstaedt, 1991; Gabric et al., 1993; Meunier et al.,

600 2012; Cropper et al., 2014). Additionally, the trapped signal is always affected by dissolution of

particular species and/groups of organisms sinking through the water column into deeper waters

602 (*e.g.*, Romero et al., 1999, 2002).

5.2. Temporal variations of the species-specific composition of the plankton community

604 We are aware that 1,900 days of continuous sampling cannot deliver a definite picture of all

temporal changes affecting the composition of the plankton community in the very dynamic

606 Mauritanian upwelling. However, the overall temporal pattern observed led us to propose a general

sequence of seasonal variability. Most of the major microorganisms' groups occur simultaneously

608   and clear successional trends are not quite distinguishable (Fig. 3). Despite strong interannual

variability (Table 4), a consistent seasonal pattern in the occurrence of species or groups of

610   species can still be recognized. Figure 4 shows the seasonal evolution of populations responding

to the temporal dynamics of nutrient availability, *e.g.* following short-period dust events (Fig. 2e)

612   and/or vertical mixing events associated with stronger winds (Fig. 7a, e). Based on the visual data

examination and the statistical analysis, four groups of species are recognized (Figs. 3, 6).

614   Populations of group 1 (Dia-bent, Dia-upw, Co-*Gocean*, OD-upw, For-cold = in blue in Fig. 6) have

higher relative contribution during the most intense phase of the upwelling season (mainly between

616   late winter/early spring and early summer; Mittelstaedt, 1983, Cropper et al., 2014). Group 1

quickly responds to intense mixing and lowered SST at the CBeu site (Fig. 7d, e) and represents

618   the typical upwelling-related association off Mauritania. This observation confirms the ecological

characterization of the species groups that has been separately presented in previous

620   biogeographical/ecological studies (Romero et al., 2002; Kucera, 2007; Köbrich et al., 2008, 2016;

Zonneveld et al., 2013; Romero and Fischer, 2017).

622   Diatoms of coastal regions (Dia-coast, non-upwelling related) and those thriving in open ocean

waters (Dia-ocean) together with other calcareous dinoflagellates (CD-other), cosmopolitan

624   organic dinoflagellate cysts (OD-cosm) and 'other coccolithophores' (Co-other) are assigned to

group 2 (in brown in Fig. 6). Except for the cosmopolitan organic dinoflagellate cysts, all

626   components of group 2 are primary producers and occur more abundantly between early fall and

late winter (Fig. 4), at times of deepening of the ML and upwelling relaxation (Fig. 7e). Group 2

628   represents a primary producer signal typical of meso- to oligotrophic waters conditions off

Mauritania, occurring under weakened upwelling, when winds predominantly blow from the N-NE,

630   SST start decreasing after their summer peak, and the uppermost water column stratifies (Fig. 7a,

d, e).

632   Except for warm waters (CD-warm) and dust input-sensitive (CD-min) calcareous dinoflagellate

cysts, group 3 is mainly composed by secondary producers: warm-water planktonic foraminifera

634   and all pteropods (Fig. 4e, f). As such, this group represents the calcareous fraction of zooplankton

feeding on (primary) phytoplankton, occurring mainly during phases of predominantly warmer

636   SSTs (Fig. 7d), N-NE-originated winds (Fig. 7a) and stratified uppermost water column (Fig. 7e).

SST appears to be the most important factor controlling assemblage composition of planktonic

638   foraminifera (Kucera, 2007). Large, symbiont-bearing specialists like *G. ruber and G. sacculifer* are

adapted to more oligotrophic and warmer waters. They show their maximum abundance in warm

640   waters with a deeper mixed-layer depth (Fig. 7e, f).

    The seasonal dynamics of group 4 is similar to that of group 3 (intervals of weakened upwelling

642   conditions), but they differ in their composition: group 4 is mainly made of calcareous primary

producers. These populations dominate the plankton community during intervals of weakened

644   upwelling, shallow MLD and predominantly oligotrophic water conditions. Similar to group 3, group

4 consists mainly of coccolithophores (the dominant *E. huxleyi*, accompanied by UPZ and LPZ, *U.*

646   *anulus*, Figs. 4b, 6), as well as organic dinoflagellate cysts characteristic for upwelling relaxation

phases (CD-upw relax). The contribution of *E. huxleyi* and accompanying coccolithophore taxa,

648   and upwelling-relaxation organic dinoflagellate cysts shows highest relative values from early fall

through early spring and decreases into the most intense upwelling season (when *G. oceanica*

650   increases, Fig. 4b). As such, this group also bears some resemblance to group 2, though coastal

and open-ocean water diatoms are component of the latter, while diatoms are absent in group 4.

652   This difference possibly reflects the distinct nutrient and water depth conditions in which *E. huxleyi*

and other coccolithophores (group 4) and diatoms (group 2) typically thrive.

654   **5.3. Shifts in the species-specific composition of assemblages between 2004 and 2006**

    The persistent seasonal pattern of the groups' and species occurrence experiences occasional

656   shifts. Several events, which altered the 'regular' pattern of temporal occurrence of species or

group species at site CBeu, were observed between late 2004 and late 2006 (Fig. 7f-j). We identify

658   three main shift stages in the species-specific composition of assemblages:

    1.   Stage 1 (2004): (*i*) low total biogenic production (summer–fall 2004, Fig. 2b-d), and (*ii*)

660   absence of warm-water foraminifera (Fig. 7f). These changes in production/flux were

accompanied by (*iii*) a significant decrease in SST as reconstructed with $U_{37}^{K\prime}$ (Fig. 7d).

662   2.   Stage 2 (late 2005/early 2006): (*i*) extraordinarily high relative contribution of the

coccolithophore *U. anulus* (Fig. 7i); as well as (*ii*) the first high occurrence of *L. bulimoides*

664   and uncoiled pteropods (Fig. 7h).

3. Stage 3 (after fall 2006): (*i*) strong increase of the relative contribution of benthic diatoms

666 (Fig. 7i) and warm-water calcareous dinoflagellates (Fig. 7j), and (*ii*) highest longest

occurrence and highest relative abundance of *L. bulimoides* (fall 2006/winter 2007, Fig.

668 7h).

A certain degree of interannual variability of the physical setting (Mittelstaedt, 1983, 1991;

670 Cropper et al., 2014) might explain the shifts in the species-specific composition of the

assemblages. The near-disappearance of warm-water planktonic foraminifera in 2004 (Fig. 7f) was

672 most probable the response to lower-than-usual water temperatures (Fig. 7d). However, the SST

decrease is not recorded by satellite imagery. The overall climate evolution indicates a longer

674 warm and dry period from 2001-2004 in the Sahel and Sahara (east of site CBeu) and

anomalously warm temperatures in the Eastern Atlantic (Zeeberg et al., 2008; Alheit et al., 2014).

676 2004 is the only year of our study with noticeable temporal discrepancies between satellite and

$U_{37}^{K\prime}$-based temperature (Fig. 7d). This temperature gap suggests a certain decoupling between the

678 temperature signal of the uppermost centimeters of the water column (satellite) and subsurface

waters where the alkenone-forming coccolithophores dwell (*E. huxleyi* and *G. oceanica*; Conte et

680 al., 1995). As planktonic foraminifera mainly react to SST variability (Kucera, 2007), cooler than

usual subsurface waters between middle winter and early fall 2004 (Fig. 7d) might have been

682 responsible for the strong decrease of the warm-water planktonic foraminifera contribution (Fig. 7f).

Additionally, all other plankton groups show lowest fluxes toward late summer. Neither the

684 seasonal pattern nor the MLD show any significant change nor unusually high lithogenic fluxes

occurred (Fig. 2e, 7e). Exceptionally, the winter season 2004/2005 is characterized by a high total

686 mass flux (Fig. 2a); this extraordinarily high seasonal value matches well with the highest fluxes of

TOC and $CaCO_3$ for the studied interval.

688 The extraordinary high relative abundance of *U. anulus* in fall 2005 has not yet been observed

in similar or other settings, although it is often listed in studies of large-scale distribution patterns of

690 coccolithophores (*e.g.*, Böckel and Baumann, 2008; Estrada et al., 2016; Poulton et al., 2017). So

far only Steinmetz (1991) has found *U. anulus* (described as *U. calvata* and *U. scituloma*) in

692 'frequent' abundances in sediment traps deployed in the equatorial Atlantic, central Pacific, and in

the Panama Basin, but without adding detailed information such as fluxes, the timing of its

694   occurrence or its ecological significance. In most of earlier trap studies, *U. anulus* has been

grouped together with other umbilicosphaerids coccolithophores, since it did not reach high

696   abundances (*e.g.*, Köbrich et al., 2016; Guerreiro et al., 2017). Nevertheless, umbilicosphaerids

seem to favor warm and more oligotrophic conditions (Baumann et al., 2016), so that the increased

698   input of tropical surface waters transported northward via the MC (Mittelstaedt, 1991) can be

possibly responsible for the advection of *U. anulus* upon the site CBeu.

700   The shift in the pteropod composition from dominating *H. inflatus* towards the appearance of *L.*

bulimoides between winter 2005 and spring 2006 –and again in fall and winter 2006/2007 (Fig.

702   7h)– can be also explained by the increased influence of warmer surface waters of southern origin.

Heliconoides inflatus is known as a rather cosmopolitan species, occurring across a wide range of

704   oceanic provinces (Bé and Gilmer, 1977; Burridge et al., 2017), whereas *L. bulimoides* seems to

prefer waters of subtropical gyres (although it was also present in low numbers in the equatorial

706   region, Burridge et al., 2017). A stronger transport of the MC from the south may have led to the

deterioration of the adequate environmental conditions for *H. inflatus*, as can be seen by the

708   extremely low total pteropods flux during winter 2005 to spring 2006 (Fig. 3e), and, thus, to the

relative enrichment of *L. bulimoides*. The fact that the latter species is absent again in winter 2008

710   (Fig. 7h) represents a gradual return to previous ('regular') winter conditions. 'Regular'

temperatures from early 2005 on allowed the reappearance of warm-water planktonic foraminifera

712   in fall 2005 (Fig. 7f).

The exceptional increase in the contribution of the benthic diatoms in spring-summer 2006 (Fig.

714   7i) might have been possibly related to the intensification of lateral advection upon the

intermediate-waters deployed CBeu trap (Romero and Fischer, 2017). Observational and model

716   experiments show that the transport of particles from the Mauritanian shelf and the uppermost

slope via nepheloid layers significantly contributes to the deposition upon the lowermost slope and

718   beyond than the direct vertical settling of particles from the surface layer (Nowald et al., 2014;

Karakaş et al., 2006; Fischer et al., 2009; Zonneveld et al., 2018). The relevance of advective

720   processes within nepheloid layers has been already proposed for similar settings (Puig and

Palanques, 1998; Inthorn et al., 2006). We speculate that the longer predominance of N-NE winds

722   between 2005 and 2007 (Fig. 7a) might have possibly intensified the transport of benthic diatoms

from the shallow coastal area into the hemipelagic CBeu trap via the MC (Fig. 1). Enhanced lateral

724 transport has important environmental implications for the final burial of organic matter in EBUEs.

As the organic matter can be effectively displaced from the area of production (Inthorn et al.,

726 2006), carbon depocenters generally occur at the continental slopes between 500 and 2,000 m. In

the CC-EBUE around Cape Blanc, the depocenter with up to 3% of organic carbon has a depth

728 range between 1,000 and 2,000m (Fischer et al., 2019).

Most of the populations affected by and responding to shifting environmental conditions off

730 Mauritania between 2004 and 2006 returned to their 'regular' seasonal pattern of occurrence after

2006 (Fig. 4). However, some shifts persisted after summer 2006. *Limacina bulimoides* still

732 dominated the pteropod assemblage (Fig. 7h), the total pteropod flux showed the highest maxima

for the entire studied interval (might be due to the large food supply and organic matter as

734 represented by high total fluxes of diatoms, Fig. 3a, e), and warm-water calcareous dinoflagellate

cysts increased during late fall 2006 (Fig. 7j). An exception to this pattern is the high relative

736 contribution of benthic diatoms (Figs. 4a, 7i; Romero and Fischer, 2017). At this stage, we cannot

fully disregarded that the shift in the species-specific composition of the diatom community (also

738 present after 2008; Romero and Fischer, 2017; Romero, unpublished observations) might be due

to the natural long-term variability due to external forcings (*e.g.*, North Atlantic Oscillation) or due to

740 on-going climate change.

Our multiannual trap experiment provides a unique opportunity to study the long-term evolution

742 of the plankton community in an ecologically important EBUE. Rapid shifts in the population

contribution at site CBeu demonstrate that calcareous, siliceous and organic plankton

744 microorganisms rapidly react to environmental changes in the CC-EBUE off Mauritania. Time-

series trap experiments continuously conducted over many years –as those currently in the CC-

746 EBUE (Fischer et al., 2016, 2019; Romero et al., 2002, 2016, 2017)– deliver a reliable

observational basis on the occurrence of long-lasting variations of populations in response to key

748 environmental forcings. Among others, our multiannual observations are useful for future model

experiments on plankton dynamics and evolution in low- and mid-latitude EBUEs and how

750 organisms influencing the global carbon cycle might react to global and ocean warming.

752   **6. Conclusions**

-    The seasonal amplitude of the flux variations of primary and secondary producers in the upper

754   water column off Mauritania was well recorded in our continuous trap experiment that lasted 1,900

days. The repeated yearly pattern of higher fluxes of diatoms, coccolithophores, organic-walled

756   dinoflagellate cysts and planktonic foraminifera between early spring and early/middle summer

matched well the temporal occurrence of the most intense upwelling interval in waters overlying

758   site CBeu. Conversely, fluxes of calcareous dinoflagellate cysts and pteropods were higher during

intervals of upwelling relaxation (late summer through late fall).

760   -   The good temporal match between maxima of (most of) studied microorganism groups and

biogenic bulk components unambiguously evidences the contribution of primary and secondary

762   producers to the total mass/biogenic mass fluxes. The notorious coupling between fluxes of

lithogenics and major microorganism groups provides compelling evidence for the biological pump

764   off Mauritania to be strongly dependent on the dust input from the Sahara/Sahel and the eolian-

transported nutrient deposition.

766   -   1,900 days of continuous trap record of microorganism fluxes allowed for the recognition of a

general sequence of seasonal variations of the main plankton populations thriving in coastal

768   waters off Mauritania. The temporal turnover (succession) was better shown by the temporal

variations of particular species or groups of species.

770   -   A significant shift in the 'regular' seasonal pattern of populations' occurrence was recognized in

species relative contributions between 2004 and 2006. Several events altering the regular

772   seasonal pattern were observed and occurred in three main stages: summer–fall 2004, late

2005/early 2006, and after fall 2006. Although most of the populations return 'to normal' after fall

774   2006, a few did not.

-    Our multiannual trap experiment emphasizes the significance of long-term records on

776   evaluating the impact of changing environmental conditions on living populations. Time-series trap

experiments conducted over many years –as those currently conducted in the CC-EBUE by

778   MARUM– deliver a broad observational basis on the occurrence of persistent seasonal and

interannual patterns. They also help in the interpretation of long-lasting variations of population

780 changes in response to key environmental forcings, such as nutrient input, water masses

variability, lateral transport and/or climate change. The applicability of the flux dynamics of primary

782 and secondary producers here presented is not limited to the Mauritanian upwelling system, and it

might comparable to other EBUEs.

784

Code and Data Availability

786 Data are available at https://doi.pangaea.de/10.1594/PANGAEA.904390

788 **Author Contributions**

All authors collected the data. Oscar E. Romero wrote the manuscript. All authors contributed to

790 results interpretation and discussion.

792 **Competing Interests**

The authors declare that they have no conflict of interest.

794

Acknowledgements

796 We are greatly indebted to the masters and crews of the RVs Poseidon and MS Merian. We

greatly appreciate the help of the RV Poseidon headquarters at Geomar (K. Lackschewitz, Kiel,

798 Germany) during the planning phases of the research expeditions and the support by the German,

Moroccan and Mauritanian authorities in Berlin, Rabat and Nouakchott. We also thank the IMROP

800 and its director at Nouadhibou (Mauritania) for their general support and the help in getting the

necessary permissions to perform our multiyear trap experiments in Mauritanian coastal waters.

802 We thank G. Ruhland, N. Nowald and M. Klann (MARUM, Bremen) for mooring deployments and

lab work on the samples. This work was possible due to the long-term funding by the German

804 Research Foundation (DFG) through SFB 261, the Research Center Ocean Margins (RCOM) and

the MARUM Excellence Cluster "The Ocean in the Earth System" (University of Bremen, Bremen,

806 Germany). V. Pospelova is the Hanse-Wissenschaftskolleg (HWK) senior research fellow in

marine and climate research at the Institute for Advanced Study (Delmenhorst, Germany). Dr.

808 Manuel Bringué and an anonymous referee are acknowledged by their very helpful reviews.

810

References

812 Alheit, J., Licandro, P., Coombs, S., Garcia, A., Giráldez, A., Santamaría, M. T. G., Slotte, A.,

Tsikliras, A.C.: Atlantic Multidecadal Oscillation (AMO) modulates dynamics of small pelagic

814 fishes and ecosystem regime shifts in the eastern North and Central Atlantic, J. Marine Syst.,

133, 88-102, 2014.

816 Anabalón, V., Arístegui, J., Morales, C.E., Andrade, I., Benavides, M., Correa-Ramírez, M. A.,

Espino, M., Ettahiri, O., Hormazabal, S., Makaoui, A., Montero, M. F., Orbi, A.: The structure of

818 planktonic communities under variable coastal upwelling conditions off Cape Ghir (31°N) in the

Canary Current System (NW Africa), Prog. Oceanogr., 120, 320-339, 2014.

820 Arístegui, J., Barton, E.C., Álvarez-Salgado, X. A., Santos, A. M. P., Figueiras, F. G., Kifani, S.,

Hernández-León, S., Mason, E., Machú, E., Demarcq, H.: Sub-regional ecosystem variability in

822 the Canary Current upwelling, Prog. Oceanogr., 83, 33–48, 2009.

Barber, R. T., Hiscock, M.R.: A rising tide lifts all phytoplankton: Growth response of other

824 phytoplankton taxa in diatom-dominated blooms, Global Biogeochem. Cy., 20, GB4S03,

doi:10.1029/2006GB002726, 2006.

826 Barton, E. D.: Eastern Boundary of the North Atlantic: Northwest Africa and Iberia, in: The Sea,

edited by Robinson A. R., Brink, K. H., 11, 633-657, 1998.

828 Baumann, K.-H., Freitag, T.: Pleistocene fluctuations in the Benguela Current system as revealed

by coccolith assemblages, Mar. Micropaleontol., 52, 195-215, 2004.

830 Baumann, K.-H., Andruleit, H., Böckel, B., Geisen, M., Kinkel, H.: The significance of extant

coccolithophores as indicators of ocean water masses, surface water temperature, and

832 paleoproductivity: a review, Paläontolog. Zeitschr., 79/1, 93-112, 2005.

Baumann, K.-H., Böckel, B.: Spatial distribution of living coccolithophores in the southwestern Gulf

834 of Mexico, J. Micropaleontol., 32, 123-133, 2013.

Baumann, K.-H., Saavedra-Pellitero, M., Böckel, B., Ott, C.: Morphometry, biogeography and

836 ecology of *Calcidiscus* and *Umbilicosphaera* in the South Atlantic, Rev. Micropaleontol., 59,

239-251, doi:10.1016/j.revmic.2016.03.001, 2016.

838   Bé, A. W. H., Gilmer, R. W.: A zoographic and taxonomic review of euthecosomatous pteropoda,

in: Oceanic Micropalaeontology, Vol. 1, edited by Ramsay, A. T. S., Academic Press, London,

840   733–808, 1977.

Böckel, B., Baumann, K.-H.: Vertical and lateral variations in coccolithophore community structure

842   across the subtropical frontal zone in the South Atlantic Ocean, Mar. Micropaleontol., 67, 255-

273, 2008.

844   Bory, A., Jeandel, C., Leblond, N., Vangriesheim, A., Khripounoff, A., Beaufort, L., Rabouille, C.,

Nicolas, E., Tachikawa, F., Etcheber, H., Buat-Ménard, P.: Downward particle fluxes within

846   different productivity regimes off the Mauritanian upwelling zone (EUMELI program), Deep-Sea

Res. I, 48, 2251-2282, 2001.

848   Bouimetarhan, I., Marret, F., Dupont, L., Zonneveld, K. A. F.: Dinoflagellate cyst distribution in

marine surface sediments off West Africa (17 – 6°N) in relation to sea-surface conditions,

850   freshwater input and seasonal coastal upwelling, Mar. Micropaleontol., 71, 113-130, 2009.

Bringué, M., Thunell, R. C., Pospelova, V., Pinckney, J. L., Romero, O. E., Tappa, E.J.: Physico-

852   chemical and biological factors influencing dinoflagellate cyst production in the Cariaco Basin,

Biogeosciences, 15, 2325–2348, 2018.

854   Bringué, M., Pospelova, V., Tappa, E. J., Thunell, R. C.: Dinoflagellate cyst production in the

Cariaco Basin: a 12.5 year-long sediment trap study, Prog. Oceanogr., 171, 175-211, 2019.

856   Buesseler, K.O., Antia, A.A., Chen, M., Fowler, S.W., Gardner, W.D., Gustafsson, O., Harada, K.,

Michaels, A.F., Rutgers van der Loeff, M., Sarin, M., Steinberg, D.K., Trull, T.: An assessment

858   of the use of sediment traps for estimating upper ocean particle fluxes, J. Mar. Res., 65, 345-

416, 2007.

860   Burridge, A. K., Goetze, E., Wall-Palmer, D., Le Double, S. L., Huisman, J., Peijnenburg, K. T. C.

A.: Diversity and abundance of pteropods and heteropods along a latitudinal gradient across the

862   Atlantic Ocean, Prog. Oceanogr., 158, 213-223, 2017.

Chavez, F. P., Messié, M.: A comparison of Eastern Boundary Upwelling Ecosystems, Prog.

864   Oceanogr., 83, 80-96, 2009.

Conte, M. H., Thompson, A., Egrinton, G., Green, J. C.: Lipid biomarker diversity in the

866   coccolithophorid *Emiliania huxleyi* (Prymnesiophyceae) and the related species *Gephyrocapsa*

oceanica, J. Phycol, 31, 272–282, 1995.

868   Conte, M. H., Sicre, M., Rühlemann, C., Weber, J. C., Schulte, S., Schulz-Bull, D., Blanz, T.:

Global temperature calibration of the alkenone unsaturation index (UK′37) in surface waters and

870   comparison with surface sediments, Geochem. Geophy. Geosy., 7(2),

https://doi.org/10.1029/2005GC001054, 2006.

872   Cropper, T. E., Hanna, E., Bigg, G. R.: Spatial and temporal seasonal trends in coastal upwelling

off Northwest Africa, 1981–2012, Deep-Sea Res. I, 86, 94-111, 2014.

874   Crosta, X., Romero, O. E., Ther, O., Schneider, R. R.: Climatically-controlled siliceous productivity

in the eastern Gulf of Guinea during the last 40 000 yr, Clim. Past., 8, 415-431, 2012.

876   Elbrächter, M., Gottschling, M., Hildebrand-Habel, T., Keupp, H., Kohring, R., Lewis, J., Meier, K.

J. S., Montresor, M., Streng, M., Versteegh, G. J. M., Willems, H., Zonneveld, K., Establishing

878   an agenda for calcareous dinoflagellate research (Thoracosphaeraceae, Dinophyceae)

including a nomenclatural synopsis of generic names, Taxon, 57, 1289-1303, 2008.

880   Estrada, M., Delgado, M., Blasco, D., Latasa, M., Cabello, A.M., Benítez-Barrios, V., Fraile-Nuez,

E., Mozetic, P., Vidal, M.: Phytoplankton across Tropical and Subtropical Regions of the

882   Atlantic, Indian and Pacific Oceans, PLoS ONE, 11, 3, e0151699. doi:10.1371/journal.

pone.0151699, 2016.

884   Fischer, G., Wefer, G.: Sampling, preparation and analysis of marine particulate matter, in: The

Analysis and Characterization of Marine Particles, Geophysical Monograph Series 63, edited by

886   Hurd, D. C., Spencer, D. W., 391-397, 1991.

Fischer, G., Donner, B., Ratmeyer, V., Davenport, R., Wefer, G.: Distinct year-to-year particle flux

888   variations off Cape Blanc during 1988–1991: Relation to $\delta^{18}O$-deduced sea-surface

temperatures and trade winds, J. Mar. Res., 54, 73–98, 1996.

890   Fischer, G., Karakaş, G.: Sinking rates and ballast composition of particles in the Atlantic Ocean:

implications for the organic carbon fluxes to the deep ocean, Biogeosciences, 6, 85-102, 2009.

892   Fischer, G., Romero, O. E., Merkel, U., Donner, B., Iversen, M., Nowald, N., Ratmeyer, V.,

Ruhland, G., Klann, M., Wefer, G.: Deep ocean mass fluxes in the coastal upwelling off

894   Mauritania from 1988 to 2012: variability on seasonal to decadal timescales, Biogeosciences,

13, 3071-3090, 2016.

896   Fischer, G., Romero, O. E., Toby, E., Iversen, M., Donner, B., Mollenhauer, G., Nowald, N.,

Ruhland, G., Klann, M., Hamady, B., Wefer, G.: Changes in the Dust-Influenced Biological

898   Carbon Pump in the Canary Current System: Implications From a Coastal and an Offshore

Sediment Trap Record Off Cape Blanc, Mauritania, Global Biogeochem. Cy., 33, 1100–1128,

900   https://doi.org/1110.1029/2019GB006194, 2019.

Friese, C. A., Hateren, J. A. V., Vogt, C., Fischer, G., Stuut, J.-B. W.: Seasonal provenance

902   changes in present-day Saharan dust collected in and off Mauritania, Atmos. Chem. Phys., 17,

10163-10193, 2017.

904   Fütterer, D. K.: The modern upwelling record off Northwest Africa, in: Coastal Upwelling, its

sediment record, Part B, Sedimentary records of ancient coastal upwelling, NATO Conference

906   Series IV, Marine Science, edited by Thiede, J., Suess, E., pp. 105-121, 1983.

Gabric, A. J., García, L., Van Camp, L., Nykjaer, L., Eifler, W., Schrimpf, W.: Offshore Export of

908   Shelf Production in the Cape Blanc (Mauritania) Giant Filament as Derived from Coastal Zone

Color Scanner Imagery, J. Geophys. Res., 98, C3, 4697-4712, 1993.

910   Guerreiro, C. V., Baumann, K.-H., Brummer, G.-J. A., Fischer, G., Korte, L. F., Merkel, U., Sá, C.,

de Stigter, H., Stuut, J.-B.: Coccolithophore fluxes in the open tropical North Atlantic: influence

912   of the Amazon river and of Saharan dust deposition, Biogeosciences, 14, 4577-4599,

https://doi.org/ 10.5194/bg-14-4577-2017, 2017.

914   Guerreiro, C. V., Baumann, K.-H., Brummer, G.-J. A., Korte, L. F., de Sá, C., Stuut, J.-B.:

Transatlantic gradients in calcifying phytoplankton (coccolithophores) fluxes, Progr. Oceanogr.,

916   176, https://doi.org/10.1016/j.pocean.2019.102140, 2019.

Hagen, E.: Northwest African upwelling scenario, Oceanol. Acta, 24 (Supplement), S113-S128,

918   2001.

Hardy, W., Marret, F., Penaud, A., le Mézo, P., Droz, L., Marsset, T., Kageyama, M.: Quantification

920   of last glacial-Holocene net primary productivity and upwelling activity in the equatorial eastern

Atlantic with a revised modern dinocyst database, Palaeogeogr. Palaeoecol., 505, 410-427.

922   2018.

Hasle, G. A., Syvertsen, E. E.: Marine diatoms, in: Identifying marine diatoms and dinoflagellates,

924   edited by Thomas, C., Academic Press, Inc. San Diego, CA, 1-385, 1996.

Hedges, J. I., Baldock, J. A., Gélinas, Y., Lee, C., Peterson, M. L., Wakeham, S. G.: The

926   biochemical and elemental compositions of marine plankton: A NMR perspective, Mar. Chem.,

78, 47–63, 2002.

928   Helmke, P., Romero, O. E., Fischer, G.: Northwest African upwelling and its effect on off-shore

organic carbon export to the deep sea, Global Biogeochem. Cycles, 19, GB4015,

930   doi:10.1029/2004GB002265, 2005.

Hemleben, C., Spindler, C., Anderson, O. R.: Modern Planktonic Foraminifera, pp. 363, New York

932   (Springer), 1989.

Holzwarth, U., Esper, O., Zonneveld, K. A. F.: Organic-walled dinoflagellate cysts as indicators of

934   oceanographic conditions and terrigenous input in the NW African upwelling region, Rev.

Palaeobot. Palyno., 159, 35-55, 2010.

936   Inthorn, M., Wagner, T., Scheeder, G., Zabel, M.: Lateral transport controls distribution, quality,

and burial of organic matter along continental slopes in high-productivity areas, Geology, 34,

938   205-208, doi: 210.1130/G22153.22151, 2006.

Iversen, M. H., Nowald, N., Ploug, H., Jackson, G. A., Fischer, G.: High resolution profiles of

940   vertical particulate organic matter export off Cape Blanc, Mauritania: Degradation processes

and ballasting effects, Deep-Sea Res. I, 57, 771-784, 2010.

942   Iversen, M. H., Ploug, H.: Ballast minerals and the sinking carbon flux in the ocean: carbon-specific

respiration rates and sinking velocity of marine snow aggregates, Biogeosciences, 7, 2613-

944   2624, 2010.

IOC-UNESCO TS129 IGMETS: What are Marine Ecological Time Series telling us about the

946   ocean? A status report, IOC Technical Series, 129. pp., 2017.

Jiménez-Quiroz, M. d. C., Cervantes-Duarte, R., Funes-Rodríguez, R., Barón-Campis, S. A.,

948   García-Romaro, F. d. J., Hernández-Trujillo, S., Hernández-Becerril, D. U., González-Armas, L.

V., Martell-Dubois, R., Cerdeira-Estrada, S., Fernández-Mémdez, J., González-Ania, L. V.,

950   Vásquez-Ortiz, M., Barrón-Barraza, F. J.: Impact of "The Blob" and "El Nino" in the SW Baja

California Peninsula: Plankton and environmental variability of Bahia Magdalena, Front. Mar.

952   Sci., 6, 1-23, 2019.

Jordan, R. W., Zhao, M., Eglinton, G., Weaver, P. P. E.: Coccolith and alkenone stratigraphy and

954   palaeoceanography at an upwelling site off NW Africa (ODP 658C) during the last 130,000

years, in: Microfossils and oceanic environments, edited by Moguilevsky, A., Whatley, R.,

956   University of Wales, Aberystwyth Press, London, pp. 111–130, 1996.

Karakaş, G., Nowald, N., Blaas, M., Marchesiello, P., Frickenhaus, S., Schlitzer, R.: High-

958   resolution modeling of sediment erosion and particle transport across the northwest African

shelf, J. Geophys. Res., 111, C06025, doi.org/10.1029/2005JC003296, 2006.

960   Karakaş, G., Nowald, N., Schäfer-Neth, C., Iversen, M., Barkmann, W., Fischer, G., Marchesiello,

P., Schlitzer, R.: Impact of particle aggregation on vertical fluxes of organic matter, Prog.

962   Oceanogr., 83, 331-341, 2009.

Köbrich, M. I., Baumann, K.-H.: Coccolithophore flux in a sediment trap off Cape Blanc (NW

964   Africa), J. Nannopl., 30, 83-96, 2008.

Köbrich, M. I., Baumann, K.-H., Fischer, G.: Seasonal and inter-annual dynamics of

966   coccolithophore fluxes from the upwelling region off Cape Blanc, Northwest Africa, J.

Micropaleontol, doi:10.1144/jmpaleo2014-024, 2016.

968   Kohn, M., Zonneveld, K. A. F.: Calcification depth and spatial distribution of *Thoracosphaera heimii*

cysts: Implications for palaeoceanographic reconstructions, Deep-Sea Res. I, 57, 1543-1560,

970   2010.

Kremling, K., Lentz, U., Zeitzschell, B., Schulz-Bull, D. E., Duinker, J. C.: New type of time-series

972   sediment trap for the reliable collection of inorganic and organic trace chemical substances,

Rev. Sci. Instrument., 67, 4360–4363, 1996.

974   Kucera, M.: Planktonic foraminifera as tracers of past oceanic environments: in, Developments in

Marine Geology, Volume 1, Proxies in Late Cenozoic Paleoceanography, edited by Hillaire–

976   Marcel, C., De Vernal, A., Elsevier, Amsterdam, 213-262, 2007.

Lange, C. B., Romero, O. E., Wefer, G., Gabric, A. J.: Offshore influence of coastal upwelling off

978   Mauritania, NW Africa, as recorded by diatoms in sediment traps at 2195 m water depth, Deep-

Sea Res. I, 45, 985-1013, 1998.

980   Lathuilière, C., Echevin, V., Levy, M.: Seasonal and intraseasonal surface chlorophyll-a variability

along the northwest African coast, J. Geophys. Res. Oceans, 13(C5), C05007,

982   doi:10.1029/2007/JC004433, 2008.

Marcello, J., Hernández-Guerra, A., Eugenio, F., Fonte, A.: Seasonal and temporal study of the

984   northwest African upwelling system, Int. J. Remote Sens., 32, 1843-1859, 2011.

Margalef, R.: On certain unifying principles in ecology, Am. Nat., 97, 357-374, 1963.

986   McKay, C. L., Filipsson, H. L., Romero, O. E., Stuut, J.-B. W., Donner, B.: Pelagic-benthic coupling

within an upwelling system of the subtropical northeast Atlantic over the last 35 ka BP., Quat.

988   Sci. Rev., 106, 299-315, 2014.

Meunier, T., Barton, E. D., Barreiro, B., Torres, R.: Upwelling filaments off Cape Blanc: interaction

990   of the NW African upwelling current and the Cape Verde frontal zone eddy field?, J. Geophys.

Res. Oceans, 117, C8, C08031, doi:10.1029/2012JC007905, 2012.

992   Mittelstaedt, E.: The upwelling area off Northwest Africa - a description of phenomena related to

coastal upwelling, Prog. Oceanogr., 12, 307-331, 1983.

994   Mittelstaedt, E.: The ocean boundary along the northwest African coast: Circulation and

oceanographic properties at the sea surface, Prog. Oceanogr., 26, 307–355, 1991.

996   Mollenhauer, G., Basse, A., Kim, J.-H., Sinninghe Damsté, J. S., Fischer, G.: A four-year record of

U^{K}_{37} - and TEX_{86}-derived sea surface temperature estimates from sinking particles in the

998   filamentous upwelling region off Cape Blanc, Mauritania, Deep-Sea Res. I, 97, 67–79, 2015.

Müller, P.J., Schneider, R. R.: An automated leaching method for the determination of opal in

1000   sediments and particulate matter, Deep-Sea Res. I, 40, 425-444, 1993.

Müller, P., Fischer, G.: A 4-year sediment trap record of alkenones from the filamentous region off

1002   Cape Blanc, NW Africa, and a comparison with distributions in underlying sediments, Deep-Sea

Res. I, 48, 1877-1903, 2001.

1004   Muller-Karger, F., Varela, R., Thunell, R., Luerssen, R., Hu, C., Walsh, J. J.: The importance of

continental margins in the global carbon cycle, Geophys. Rese. Lett., 32, L01602,

1006   doi:01610.01029/02004GL021346, 021341_021341-021341_021344, 2005.

Nicholson, S. E.: The West African Sahel. A review of recent studies on the rainfall regime and its

1008   interannual variability. ISRN Meteorology, 453521, doi:10.1155/2013/453521, 2013.

Nowald, N., Iversen, M. H., Fischer, G., Ratmeyer, V., Wefer, G.: Time series of in-situ particle

1010   properties and sediment trap fluxes in the coastal upwelling filament off Cape Blanc, Mauritania,

Prog. Oceanogr., 137, 1-11, 2014.

1012 Pauly, D., Christensen, V.: Primary production required to sustain global fisheries, Nature, 374, 255-257, 1995.

1014 Pelegrí, J. L., Marrero-Díaz, A., Ratsimandresy, A. W.: Nutrient irrigation of the North Atlantic, Prog. Oceanogr., 70, 366-406, 2006.

1016 Pelegrí, J. L., Peña-Isquierdo, J., Machin, F., Meiners, C., Presas-Navarro, C.: Oceanography of the Cape Verde Basin and Mauritanian Slope Waters, in Research of Marine Biodiversity and

1018 Habitats in the Northwest African Margin 3, pp. 119-153, doi 10.1007/978-94-024-1023-5_3, Berlin: Springer. 2017

1020 Pospelova, V., Zonneveld, K. A. F., Heikkilä, M., Bringué, M., Price, A. M., Esenkulova, S., Matsuoka, K.: Seasonal, annual, and inter-annual *Spiniferites* cyst production: a review of

1022 sediment trap studies, Palynology, 42, 1, 162-182, 2018.

Poulton, A. J., Holligan, P. M., Charalampopoulou, A., Adey, T. R.: Coccolithophore ecology in the

1024 tropical and subtropical Atlantic Ocean: New perspectives from the Atlantic meridional transect (AMT) Programme, Progr. Oceanogr., 158, 150-170, 2017.

1026 Prahl, F. G., Wakeham, S. G.: Calibration of unsaturation patterns in long-chain ketone compositions for palaeotemperature assessment, Nature, 330, 367-369, 1987.

1028 Puig, P., Palanques, A.: Nepheloid structure and hydrographic control on the Barcelona continental margin, northwestern Mediterranean, Mar. Geol., 149, 39–54, 1998.

1030 Rembauville, M., Meilland, J., Ziveri, P., Schiebel, R., Blain, S., Salter, I.: Planktic foraminifer and coccolith contribution to carbonate export fluxes over the central Kerguelen Plateau, Deep-Sea

1032 Res. I, 111, 91–101, https://doi.org/10.1016/j.dsr.2016.02.017, 2016.

Richter, D., Vink, A., Zonneveld, K. A. F., Kuhlman, H., Willems, H.: Calcareous dinoflagellate cyst

1034 distributions in surface sediments from upwelling areas off NW Africa, and their relationships with environmental parameters of the upper water column, Mar. Micropal., 63, 201–228, 2007.

1036 Roelke, D.L., Spatharis, S.: Phytoplankton succession in recurrently fluctuating environments, PLoS One, 10, e0121392, 2015.

1038 Romero, O. E., Lange, C. B., Fischer, G., Treppke, U.F., Wefer, G.: Variability in export production documented by downward fluxes and species composition of marine planktonic diatoms:

1040 Observations from the tropical and equatorial Atlantic, in Use of Proxies in Paleoceanography,

Examples from the South Atlantic, edited by Fischer, G., Wefer, G., Springer Verlag, Berlin,

1042   Heidelberg, 365-392, 1999.

Romero, O. E., Lange, C.B., Wefer, G.: Interannual variability (1988-1991) of siliceous

1044   phytoplankton fluxes off northwest Africa, J. Plank. Res., 24, 10, 1035-1046,

doi:1010.1093/plankt/1024.1010.1035, 2002.

1046   Romero, O. E., Dupont, L., Wyputta, U., Jahns, S., Wefer, G.: Temporal variability of fluxes of

eolian-transported freshwater diatoms, phytoliths, and pollen grains off Cape Blanc as reflection

1048   of land-atmosphere-ocean interactions in northwest Africa, J. Geophys. Res. Oceans, 108, C5,

3153, doi:10.1029/2000JC000375002003, 2003.

1050   Romero, O. E., Armand, L. K., Crosta, X., Pichon, J.-J.: The biogeography of major diatom taxa in

Southern Ocean surface sediments: 3. Tropical/Subtropical species, Palaeogeogr. Palaeocl.,

1052   223, 49-65, 2005.

Romero, O. E., Kim, J., Donner, B.: Submillennial-to-millennial variability of diatom production off

1054   Mauritania, NW Africa, during the last glacial cycle, Paleoceanography, 23, PA3218,

doi:10.1029/2008PA001601, 2008.

1056   Romero, O. E., Thunell, R. C., Astor, Y., Varela, R.: Seasonal and interannual dynamics in diatom

production in the Cariaco Basin, Venezuela, Deep-Sea Res. I, 56, 571-581, 2009a.

1058   Romero, O. E., Rixen, T., Herunadi, B.: Effects of hydrographic and climatic forcing on diatom

production and export in the tropical southeastern Indian Ocean, Mar. Ecol. Prog. Ser., 384, 69-

1060   82, 2009b.

Romero, O. E., Armand, L. K.: Marine diatoms as indicators of modern changes in oceanographic

1062   conditions, in: The Diatoms, Applications for the Environmental and Earth Sciences (Second

Edition), edited by Smol, J. P., Stoermer, E. F., Cambridge University Press, Cambridge, 373-

1064   400, 2010.

Romero, O. E., Crosta, X., Kim, J.-H., Pichevin, L., Crespin, J.: Rapid longitudinal migrations of the

1066   filament front off Namibia (SE Atlantic) during the past 70 kyr, Global Planet. Changes, 125,1-

12, http://dx.doi.org/10.1016/j.gloplacha.2014.1012.1001, 2015.

1068   Romero, O. E., Fischer, G., Karstensen, J., Cermeño, P.: Eddies as trigger for diatom productivity

in the open-ocean Northeast Atlantic, Prog. Oceanogr., 147, 38-48, 2016.

1070   Romero, O. E., Fischer, G.: Shift in the species composition of the diatom community in the eutrophic Mauritanian coastal upwelling: Results from a multi-year sediment trap experiment

1072   (2003 – 2010), Prog. Oceanogr., 159, 31-44, 2017.

Round, F. E., Crawford, R.M., Mann, D. G.: The diatoms, Cambridge University Press, Cambridge,

1074   pp. 747,1990.

Sancetta, C., Calvert, S. E.: The annual cycle of sedimentation in Saanich Inlet, British Columbia:

1076   implications for the interpretation of diatom fossil assemblages, Deep-Sea Res., 35, 1, 71-90, 1988.

1078   Schlüter, M. H., Kraberg, A., Wiltshire, K. H.: Long-term changes in the seasonality of selected diatoms related to grazers and environmental conditions, J. Sea Res., 67, 91-97, 2012.

1080   Schiebel, R., Hemleben, C.: Planktic Foraminifers in the Modern Ocean, Springer-Verlag GmbH Berlin, Heidelberg, 2017.

1082   Schrader, H.-J., Gersonde, R.: Diatoms and silicoflagellates, In: Micropaleontological counting methods and techniques - an exercise on an eight meter section of the Lower Pliocene of Capo

1084   Rosello, Sicily, edited by Zachariasse, W. J., Riedel, W. R., Sanfilippo, A., Schmidt, R. R., Brolsma, M. J., Schrader, H., Gersonde, R., Drooger, M. M., Broekman, J. A, Utrecht

1086   Micropaleontological Bulletin, Utrecht, 17, 129-176, 1978.

Siegel, D. A., Deuser, W. G.: Trajectories of sinking particles in the Sargasso Sea: modeling of

1088   statistical funnels above deep-ocean sediment traps, Deep-Sea Res. I, 44, 1519–1541, 1997.

Siggelkow, D., Vink, A., Willems, H.: Calcareous dinoflagellate cyst production, vertical transport

1090   and preservation off Cape Blanc during 1990: a sediment-trap study, J. Nannoplankton Res., 24, 160, 2002.

1092   Skonieczny, C., Bory, A., Bout-Roumazeilles, V., Abouchami, W., Galer, S. J. G., Crosta, X., Diallo, A., Ndiaye, T.: A three-year time series of mineral dust deposits on the West African

1094   margin: Sedimentological and geochemical signatures and implications for interpretation of marine paleo-dust records, Earth Planet. Sc. Lett., 364, 145-156, 2013.

1096   Smayda, T. J.: Ecological features of harmful algal blooms in coastal upwelling ecosystems, African J. Mar. Sci., 219-253, 2010.

1098   Smayda, T. J., Trainer, V. L.: Dinoflagellate blooms in upwelling systems: Seeding, variability, and

contrasts with diatom bloom behavior, Prog. Oceanogr., 85, 92-107, 2010.

1100   Smilauer, P., Leps, J.: Multivariate analysis of ecological data using Canoco 5, Cambridge

University Press, Cambridge, 1-362, 2014.

1102   Steinmetz, J. C.: Calcareous nannoplankton biocoenosis: sediment trap studies in the Equatorial

Atlantic, Central Pacific, and Panama Basin, Woods Hole Oceanographic Institution, U.S.A., 1,

1104   1-85, 1991.

Susek, E., Zonneveld, K. A. F., Fischer, G., Versteegh, G. J., Willems, H.: Organic-walled

1106   dinoflagellate cyst production in relation to upwelling intensity and lithogenic influx in the Cape

Blanc region (off north-west Africa), Phycol. Res., 53, 97-112, 2005.

1108   ter Braak, C.J., Smilauer, P.: Canoco 5. Biometris, Wageningen, pp. 1-496, 2012.

Trainer, V. L., Pitcher, G. C., Reguera, B., Smayda, T. J.: The distribution and impacts of harmful

1110   algal bloom species in eastern boundary upwelling systems, Prog. Oceanogr., 85, 33-52, 2010.

Van Camp, L., Nykjær, L., Mittelstaedt, E., Schlittenhardt, P.: Upwelling and boundary circulation

1112   off Northwest Africa as depicted by infrared and visible satellite observations, Prog. Oceanogr.,

26, 357–402, 1991.

1114   van der Jagt, H., Friese, C., Stuut, J.-B W., Fischer, G., Iversen, M.: The ballasting effect of

Saharan dust deposition on aggregate dynamics and carbon export: Aggregation, settling, and

1116   scavenging potential of marine snow, Limnol. Oceanogr., 63, 1386-1394, 2018.

Vink, A., Brune, A., Höll, C., Zonneveld, K. A. F., Willems, H.: On the response of calcareous

1118   dinoflagellates to oligotrophy and stratification of the upper water column in the equatorial

Atlantic Ocean, Palaeogeogr., Palaeoecol., 178, 53-66, 2002.

1120   Weiser, J., Baumann, K.-H., Hahn, A., Zabel, M.: Late Holocene paleoceanographic changes off

south-western Africa as inferred from nannofossil assemblages, J. Nannoplankton Res., 36, 2,

1122   161-171, 2016.

WoRMS Editorial Board, http://www.marinespecies.org, 2017.

1124   Young, J., Geisen, M., Cross, L., Kleijne, A., Sprengel, C., Probert, I., Østergaard, J.: A guide to

extant coccolithophore taxonomy, J. Nannoplankton Res., Special Issue 1, International

1126   Nannoplankton Association, 124 pp., 2003.

Young, J. R., Bown P. R., Lees J. A.: Nannotax3 website. International Nannoplankton

1128   Association. Accessed April 2019. URL: http://www.mikrotax.org/Nannotax3, 2019.

Zeeberg, J., Corten, A., Tjoe-Awie, P., Coca, J., Hamady, B.: Climate modulates the effects

1130   of *Sardinella aurita* fisheries off Northwest Africa, Fish. Res., 89, 65–75, 2008.

Zenk, W., Klein, B., Schröder, M.: Cape Verde Frontal Zone, Deep-Sea Res., 38, Suppl. 1, S505–

1132   S530, 1991.

Zonneveld, K. A. F., Susek, E., Fischer, G.: Seasonal variability of the organic-walled dinoflagellate

1134   cyst production in the coastal upwelling region off Cape Blanc (Mauritania): a five-year survey,

J. Phycol., 46, 202-215, 2010.

1136   Zonneveld, K. A. F., Chen, L., Elshanawany, R., Fischer, H. W., Hoins, M., Ibrahim, M. I.,

Pittauerova, D., Versteegh, G. J.: The use of dinoflagellate cysts to separate human-induced

1138   from natural variability in the trophic state of the Po River discharge plume over the last two

centuries, Mar. Pollut. Bull., 64, 114-132, 2012.

1140   Zonneveld, K. A. F., Marret, F., Versteegh, G. J. M., Bogus, K., Bonnet, S., Bouimetarhan, I.,

Crouch, E., de Vernal, A., Elshanawany, R., Edwards, L., Esper, O., Forke, S., Grøsfjeld, K.,

1142   Henry, M., Holzwarth, U., Kielt, J.-F., Kim, S.-Y., Ladouceur, S., Ledu, D., Chen, L., Limoges,

A., Londeix, L., Lu, H., Mahmoud, M. S., Marino, G., Matsouka, K., Matthiessen, J., Mildenhal,

1144   C., Mudie, P., Neil, L., Pospelova, V., Qi, Y., Radi, T., Richerol, T., Rochon, A., Sangiorgi, F.,

Solignac, S., Turon, J.-L., Verleye, T., Wang, Y., Wang, Z., Young, M.: Atlas of modern

1146   dinoflagellate cyst distribution based on 2405 datapoints, Rev. Palaeobot. Palynol., 191, 1-197,

2013.

1148   Zonneveld, K. A. F., Pospelova, V.: A determination key for modern dinoflagellate cysts, Palyno-

logy, 39, 387-409, 2015.

1150   Zonneveld, K. A. F., Ebersbach, F., Maeke, M., Versteegh, G. J. M.: Transport of organic-walled

dinoflagellate cysts in nepheloid layers off Cape Blanc (N-W Africa), Deep Sea Res. I, 139,

1152   55-67, 2018.

1154

1156

Figures

1158
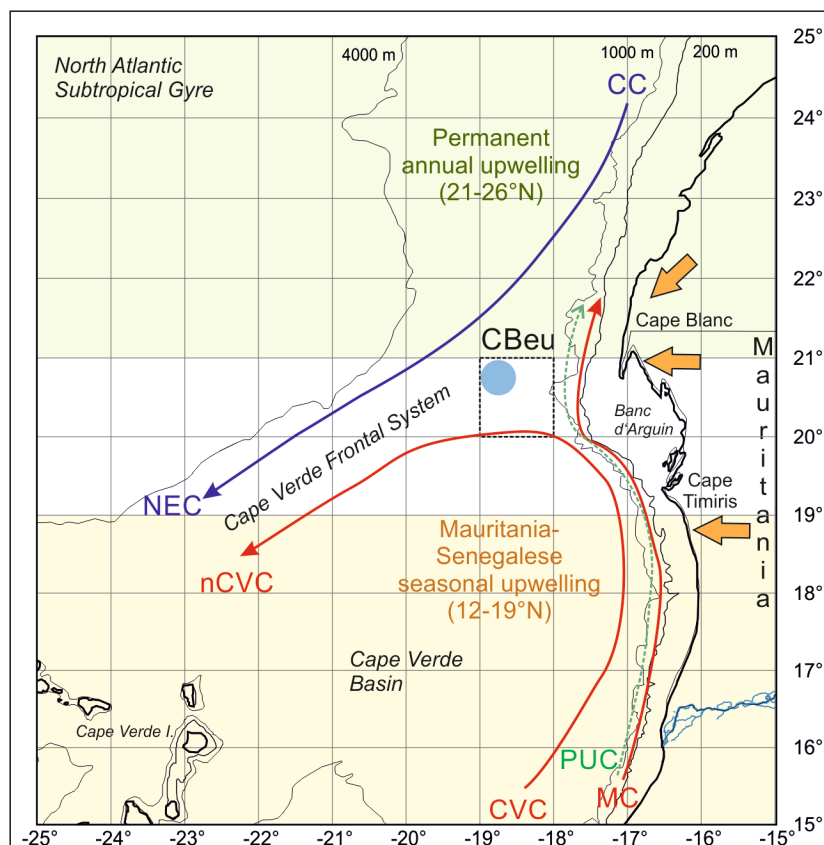
Figure 1. Map of the study area showing the location of trap site CBeu (full light blue dot), surface

1160   currents, and main wind system. Surface currents (Canary Current, CC, violet line; North

Equatorial Counter Current, blue arrow; Mauritanian Current; red arrow), North Equatorial

1162   Current (NEC), Cape Verde Current (CVC), north Cape Verde Current (nCVC), PUC are

depicted after Mittelstaedt (1983, 1991) and Zenk et al. (1991). The Cape Verde Frontal Zone

1164   (CVFZ) builds at the confluence of the NACW and the SACW (Zenk et al., 1991). Trade winds

and Saharan Air Layer are represented by orange arrows (Nicholson, 2013). The upwelling

1166   zones are depicted after Cropper et al. (2014).

1168

1170

1172

1174

1176

1178
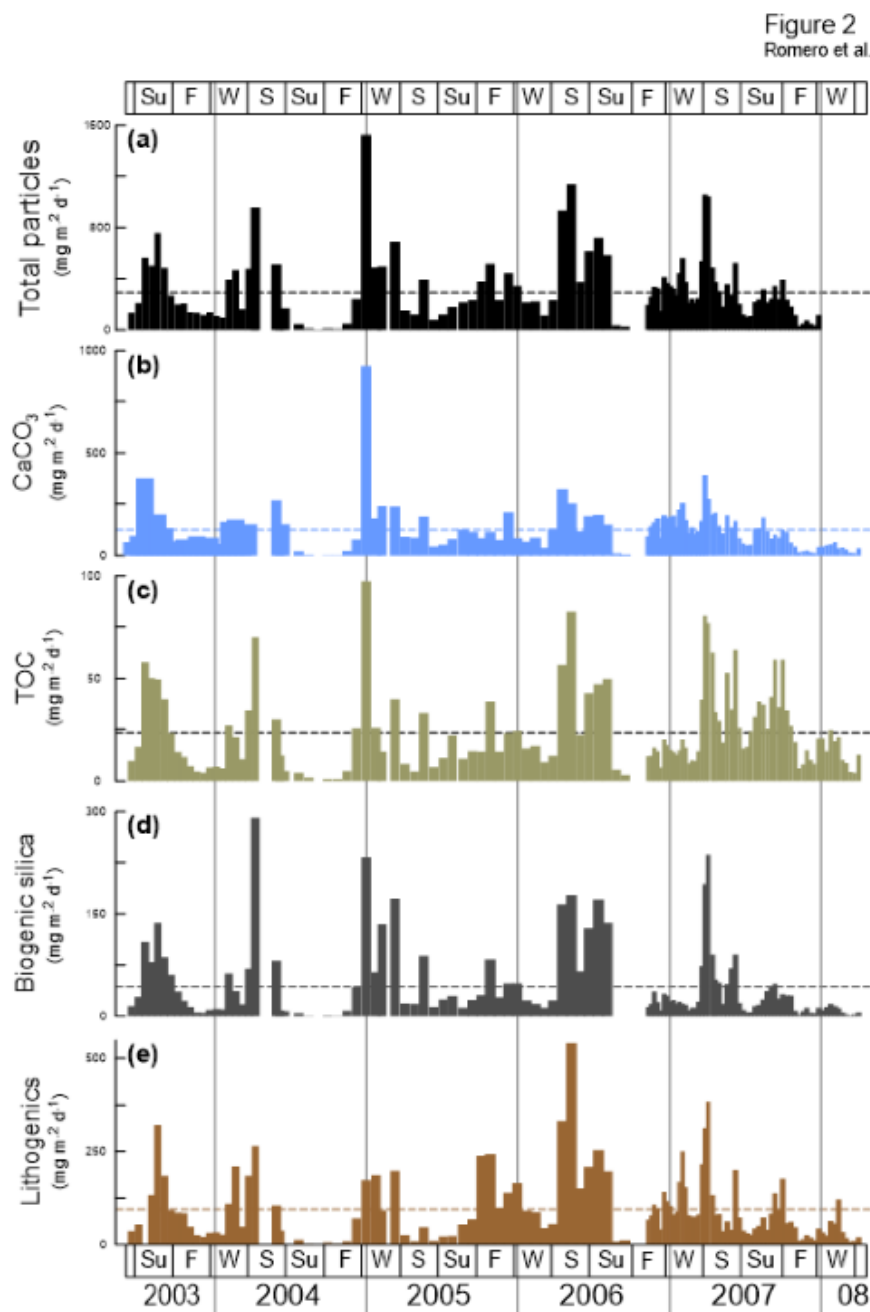
Figure 2. Total mass particle and bulk fluxes at the trap site CBeu between June 2003 and March 2008. From top to bottom: (a) total mass particle (mg m^{-2} d^{-1}, black bars), (b) calcium carbonate (CaCO$_3$, mg m^{-2} d^{-1}, light blue bars), (c) total organic carbon (TOC, mg m^{-2} d^{-1}, olive bars), (d) biogenic silica (BSi, opal, mg m^{-2} d^{-1}, dark grey bars), and (e) lithogenics (mg m^{-2} d^{-1}, brown bars). The horizontal stripped line for each parameter represents the average flux for the whole studied interval (Table 1). The boxes in the upper and lower panels represent seasons (Su=summer, F=fall, W=winter, S=spring). The vertical background gray lines indicate calendar year separation. For interpretation of the references to color in this figure legend, the reader is referred to the web version of this article.
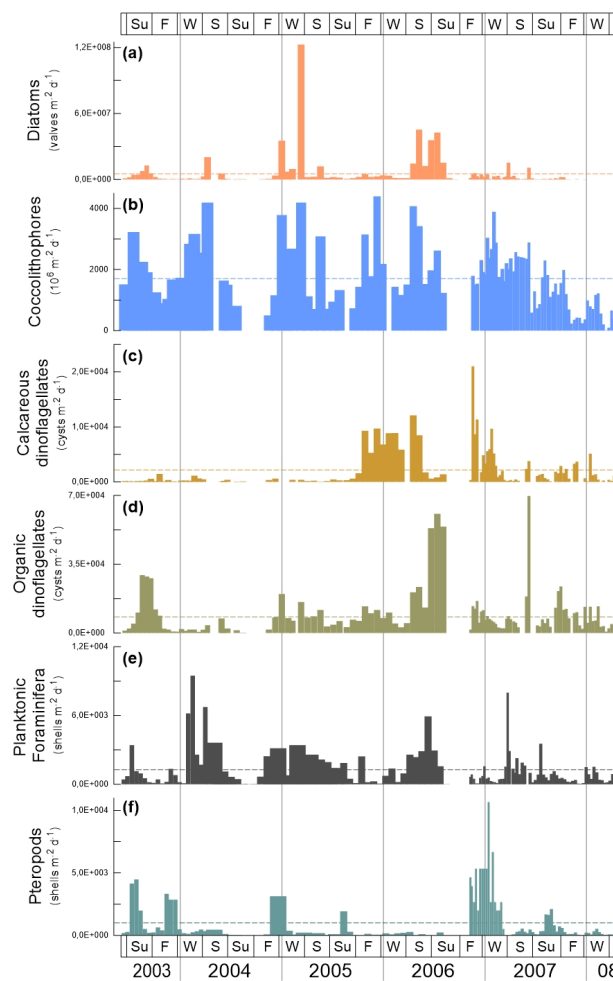
Figure 3. Fluxes of microorganisms at the trap site CBeu between June 2003 and March 2008. From top to bottom: (a) diatoms (valves m^{-2} d^{-1}, peach bars; note that ten samples corresponding to CBeu 5 –12/13/2007 through 03/17/2008– were not available for diatom analysis); (b) coccolithophores (coccoliths m^{-2} d^{-1}, light blue bars); (c) calcareous dinoflagellates (cysts m^{-2} d^{-1}; gold bars); (d) organic dinoflagellates (cysts m^{-2} d^{-1}; khaki bars); (f) planktonic foraminifera (shells m^{-2} d^{-1}; grey bars), and (f) pteropods (shells m^{-2} d^{-1}; ocean green bars). The horizontal stripped line for each group of organisms represents the average flux for the whole study interval. The boxes in the upper and lower panels represent seasons (Su=summer, F=fall, W=winter, S=spring). The vertical background gray lines indicate calendar year separation. For interpretation of the references to color in this figure legend, the reader is referred to the web version of this article.
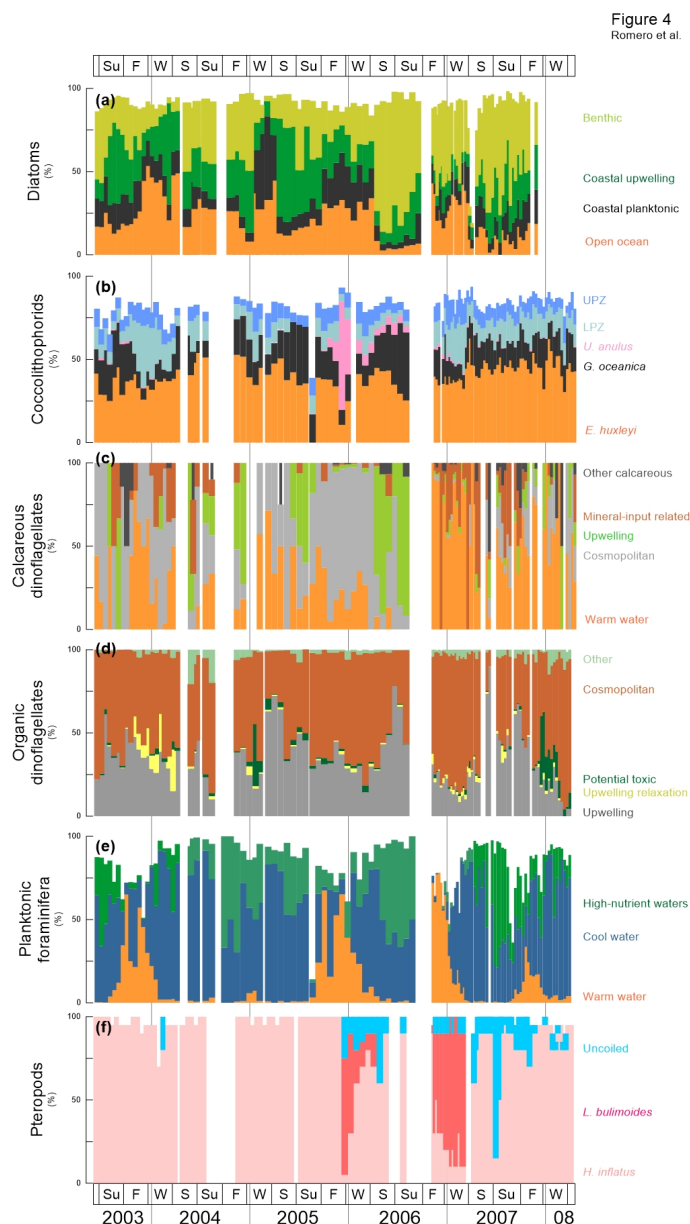
Figure 4. Cumulative relative abundance (%) of main species or group of species of diatoms, coccolithophores, dinoflagellates, planktonic foraminifera and pteropods at the trap site CBeu between June 2003 and March 2008 (Table 1). From top to bottom: (a) diatoms - benthic, light green bars; coastal upwelling, dark green bars; coastal planktonic, black bars; and open-ocean (%, orange bars; note that ten samples corresponding to CBeu 5 –12/13/2007 through 03/17/2008– were not available for diatom analysis); (b) coccolithophores –upper photic zone, blue bars; lower photic zone, moss green; *Umbilicosphaera anulus*, pink bars; *Gephyrocapsa oceanica*, black bars; *Emiliana huxleyi*, orange bars; (c) calcareous dinoflagellates – other calcareous, dark grey bars; mineral-input related, brown bars; upwelling, light green bars; cosmopolitan, light grey; warm water, orange bars; (d) organic dinoflagellates – upwelling

1214   species (grey bars); upwelling relaxation species (light yellow bars); potential toxic (dark green

       bars); cosmopolitan, red brown bars; other, faded green bars; (e) planktic foraminifera – high

1216   nutrient water, green bars; cool water, blue bars; warm water, orange bars; and (f) pteropods –

       uncoiled species, light blue bars; *Limacina bulimoides*, red bars; *Heliconoides inflatus*, pink

1218   bars. Note that the relative contribution of diatoms, coccolithophores and planktonic foraminifera

       does not add up to 100% since the ecology of some taxa of these groups is not well known

1220   constrained. The species-specific composition of groups is presented in Table 5. The boxes in

       the upper and lower panels represent seasons (Su=summer, F=fall, W=winter, S=spring). The

1222   vertical background gray lines indicate calendar year separation. For interpretation of the

       references to color in this figure legend, the reader is referred to the web version of this article.

1224

Figure 5
Romero et al.

1226
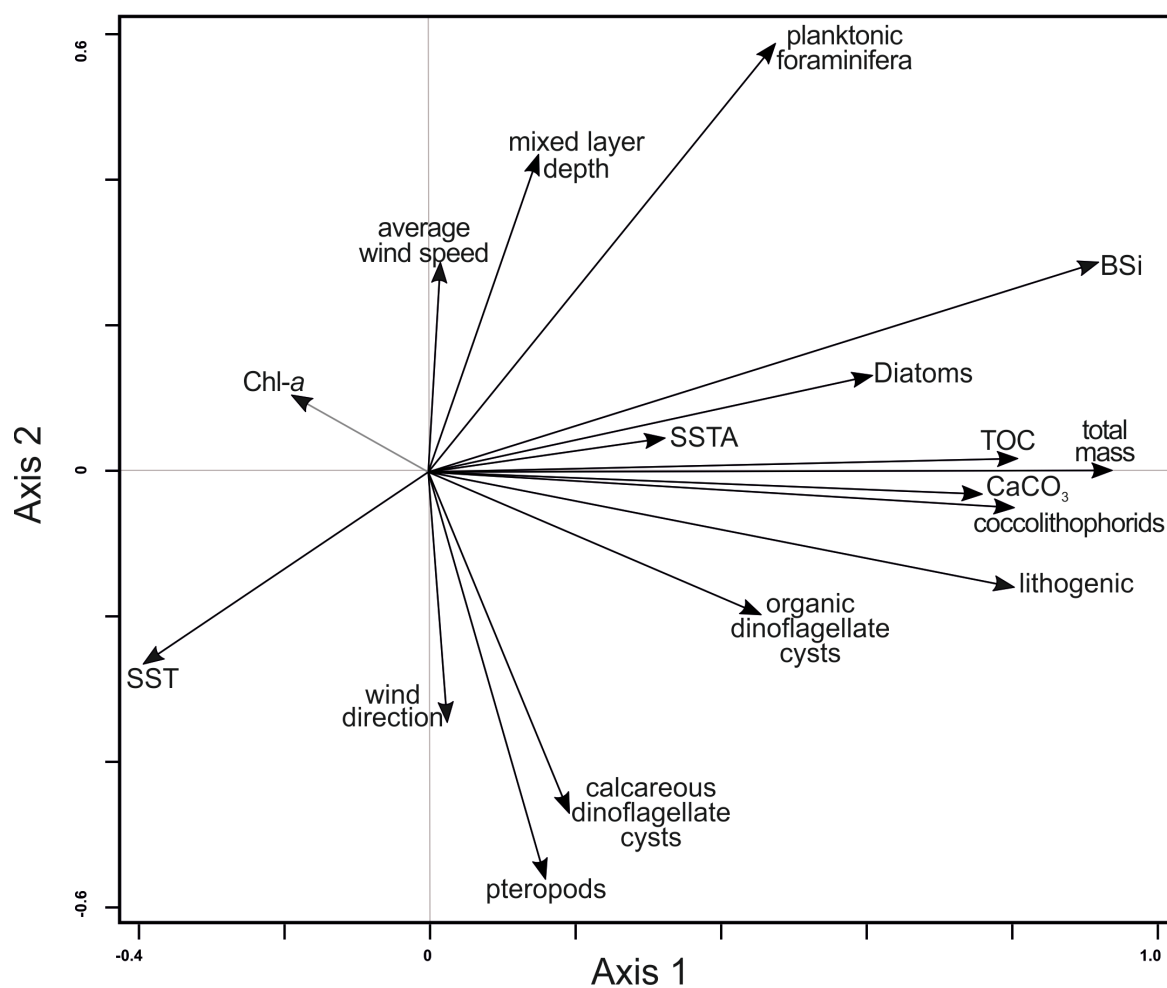
1228   Figure 5. RDA ordination diagram depicting the relationship between the accumulation rates of

        organism groups and bulk fluxes and environmental conditions in upper waters. References: Av.

1230   wind speed=average wind speed; Chl-*a*=chlorophyll *a*; TOC=total organic carbon;

        CaCO$_3$=calcium carbonate; MLD=mixed layer depth; SST=sea surface temperature; SSTA=sea

1232   surface temperature anomalies. For interpretation of the references to color in this figure legend,

        the reader is referred to the web version of this article.

1234
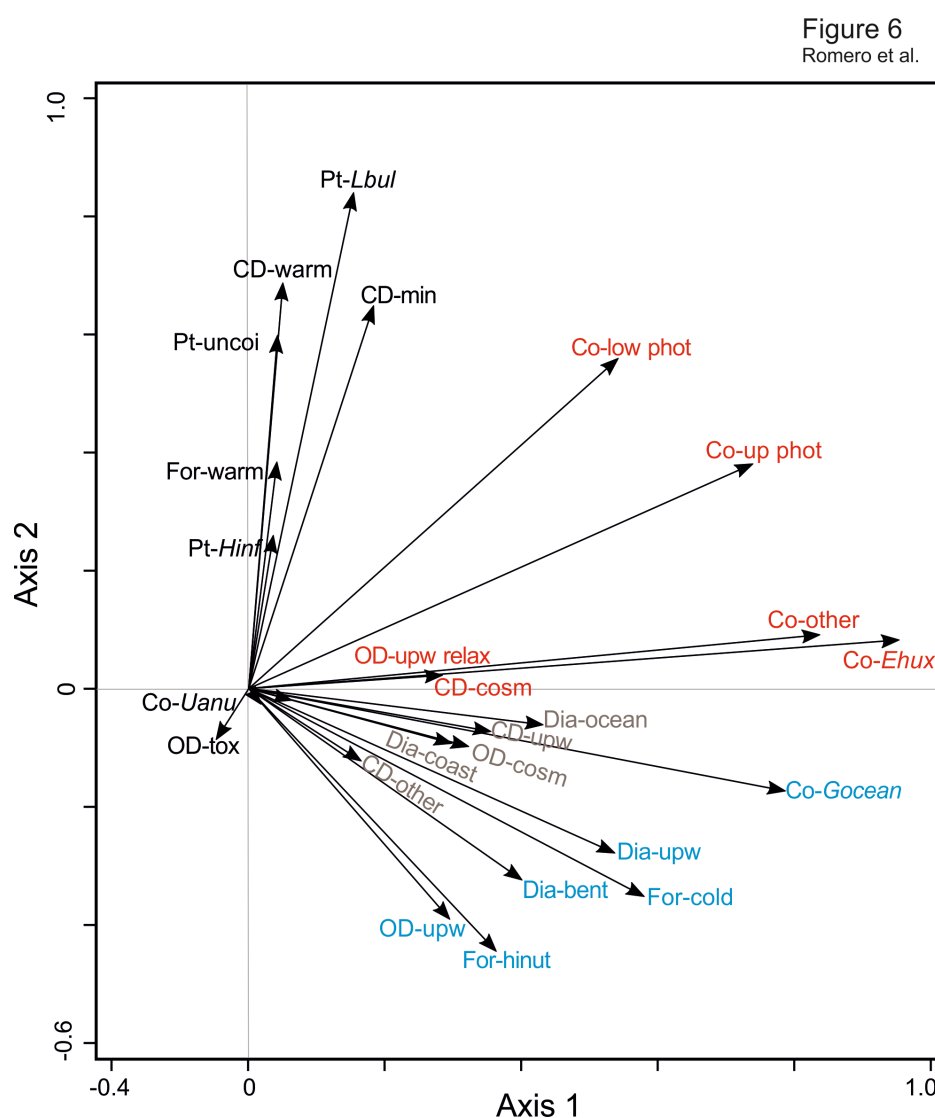
1236   Figure 6. Results of a PCA analysis of ecological groups of the organism groups at the CBeu trap

        site between June 2003 and March 2008. References: Dia (diatoms): -bent = benthic, -coast =

1238   coastal planktonic, -ocean = open ocean, -upw = upwelling; Co (coccolithophores): -*Ehux* =

        Emiliana huxleyi, -*Gocean* = *Gephyrocapsa oceanica*, -low phot: low photic zone, -other: other

1240   coccolithophroids, -*Uanu* = *Umbilicosphaera anulus,* -up phot: upper photic zone; CD (calcareous

dinoflagellate cysts): -cosm = cosmopolitan group, -min = terrestrial mineral group, -other =

1242   species that do not fit in one of the other ecological groups, -upw = upwelling, warm: warm

waters; OD (organic-walled dinoflagellate cysts): -cosm = cosmopolitan group, -other = species

1244   that do not fit in one of the other ecological groups, -tox = potential toxic group, -upw = upwelling,

-upw relax = upwelling relaxation; For (plantonic foraminifera): -cold: cold water group, -hinut =

1246   high nutrient waters group; -warm = warm water group; and Pt (pteropods): *-Hinf = Heliconoides*

inflatus, *-Lbul = Limacina bulimoides*, -uncoi: uncoiled. Groups of microorganisms are identified

1248   by colors (light blue, group 1; brown, group 2; black, group 3; and red, group 4). The species-

specific composition of groups is presented in Table 5. For interpretation of the references to

1250   color in this figure legend, the reader is referred to the web version of this article.

1252
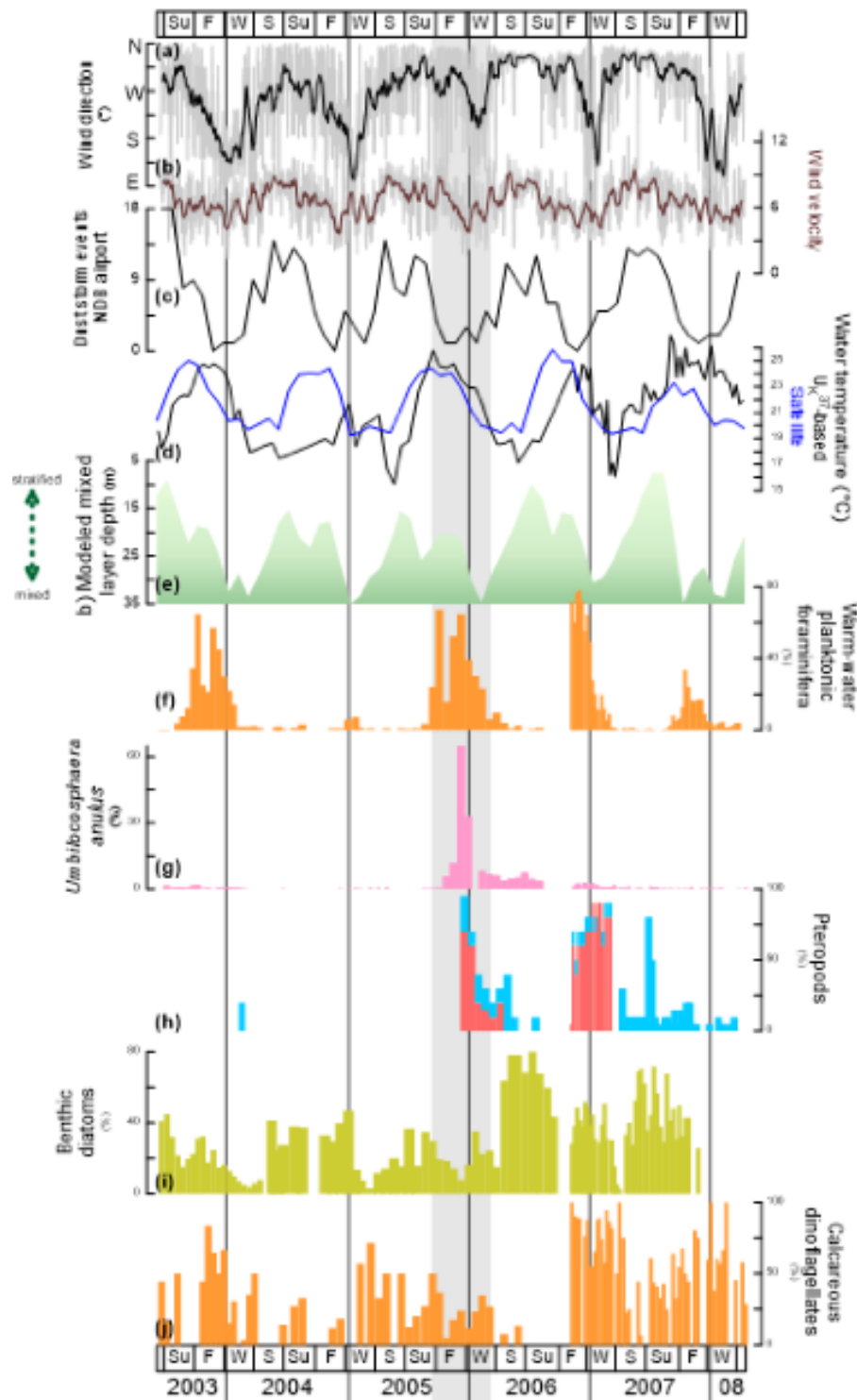
1254 Figure 7. Comparison physical data (a-e) and relative abundance of selected species or group/s of

species (f-j) at site CBeu between June 2003 and March 2008. Physical data: (a) origin of daily

1256 wind direction (the grey line are daily data, the thicker black line represent the 17-running point

average); (b) daily wind velocity (m s^{-1}, the grey line are daily data, the thicker dark brown line

1258 represent the 17-running point average), (c) dust storm event (number of events) recorded at the

meteorological station of the Airport of Nouadhibou (ca. 20°57'N, 17°02'W, Mauritania); (d)

seawater temperature (°C): $U_{37}^{K'}$-based reconstruction (black line) and satellite-imagery generated

data (blue line); (e) mixed layer depth (m, grey line, https://modis.gsfc.nasa.gov for the area

between 19°-18°W and 20°-21°N). Relative contribution (%) of (f) warm-water planktonic

foraminifera (orange bars); (g) the coccolithophore *A. anulus* (pink bars); (h) pteropods *L.*

bulimoides (red bars) and uncoiled species (light blue bars); (i) benthic diatoms (banana yellow

bars); and (j) calcareous dinoflagellates (light orange bars)*.* The species-specific composition of

groups is presented in Table 5. The vertical gray lines indicate years separation. The light grey

shading in the background highlights the interval of main shift in fluxes values and/or the relative

contribution of particular species or group of species (see discussion in 5.3.). For interpretation of

the references to color in this figure legend, the reader is referred to the web version of this

article.

1288 **Tables**

Table 1 – Romero et al.

1290

Mooring CB$_{eu}$	Coordinates	GeoB-#/ cruise	Trap depth (m)	Ocean bottom depth (m)	Sample amount	Capture duration (sample/days)	Sampling interval
1	20°45'N 18°42'W	- POS 310	1,296	2,714	20	1 = 10.5, 2-20 = 15.5	06/05/2003 – 04/05/2004
2	20°45'N 18°42'W	9630-2 M 65-2	1,296	2,714	20	1-20 = 22, 2-19 = 23	04/18/2004 – 07/20/2005
3	20°45.5'N 18°41.9'W	11404-3 POS 344-	1,277	2,693	20	21.5	07/25/05 – 09/28/2006
4	20°45.7'N 18°42.4'W	11835-2 MSM 04b	1,256	2,705	20	1 = 3.5, 2-20 = 7.5	10/28/2006 – 03/23/2007
5	20°44.9'N 18°42.7'W	12910-2 POS 365-	1,263	2,709	38	1, 2 = 6.5, 3-38 = 9.5	03/28/2007 – 03/17/2008

Table 1: Data deployment at site CBeu (Cape Blanc eutrophic, off Mauritania): coordinates, GeoB

1292 location and cruise, trap depth, ocean bottom depth, sample amount, capture duration of each

sample and sampling interval. Two gaps in the sampling intervals occurred: 04/05/2004–

1294 04/18/2004, and 09/28/2006–10/28/2006.

Table 2   Romero et al.

Analysis	Method	Analysed Parameters	Length of gradient	Eigenvalue Axis 1 (%)	Eigenvalue Axis 2 (%)	Eigenvalue Axis 3 (%)	Eigenvalue Axis 4 (%)	P-value
1	RDA	Fluxes of microoorganisms and bulk parameters, environmental parameters	1.8	34.5	10.7	4.7	2.1	0.002
2	PCA	microorganisms	1.4	26.3	16.2	9.8	6.9	

1296   References: RDA, Redundancy Analysis; PDA, Principal Component Analysis.

Table 2: Main result values of the ordination techniques Redundancy (RDA) and Principal

1298 Component (PCA) analyses performed with the software Package Canoco 5 (ter Braak and

Smilauer, 2012; Smilauer and Leps, 2014).

1300

Table 3

Romero et al.

Year	Total mass	CaCO3		TOC		Biogenic silica		Lithogenics	
	(mg m-2 d-1)	(mg m-2 d-1)	(%)	(mg m-2 d-1)	(%)	(mg m-2 d-1)	(%)	(mg m-2 d-1)	(%)
2004	309.5+403.9	150.9+360.2	48.75	21.93+39.7	7.15	54.61+85.6	17.57	84.6+66.5	27.33
2005	317.5+176.6	125.5+65.3	39.45	19.00+11.00	6.00	52,4+46.2	16.50	101.7+82.5	32.03
2006	377.9+281.9	142.8+79.1	37.79	23.3+20.6	6.19	54.07+60.2	14.31	134.2+122.6	35.51
2007	282.8+225.1	121.1+80.2	42.18	29.4+19.6	10.38	35.8+46.9	12.66	92.9+83.4	32.85

Table 3: Average daily fluxes of total mass, calcium carbonate ($CaCO_3$), total organic carbon (TOC), biogenic silica and lithogenics (mg m^{-2} d^{-1}) calculated at site CBeu for full calendar years 2004, 2005, 2006 and 2007.

Table 4

Year	Diatoms					Coccolithophores						Calcareous dinoflagellate cysts						Organic di...	
	Flux	Benthic	Coastal upwelling	Coastal planktonic	Open-ocean	Flux	E huxleyi	G. oceanica	Low photic zone	Upper photic zone	A. anulus	Flux	Other calcareous	Mineral input	Upwelling	Cosmopolitan	Warm waters	Flux	Upwelling
	(valves m^{-2} d^{-1})	Relative abundance (%)				(coccoliths *10^6 m^{-2} d^{-1})	Relative abundance (%)					(cysts m^{-2} d^{-1})	Relative abundance (%)					(cysts m^{-2} d^{-1})	
2004	4770323+14831598	23.96+15.54	27.56+10.95	27.56+10.95	27.56+10.95	2094+1159	43.73+6.70	14.77+7.98	13.86+2.21	6.72+1.92	0.14+0.18	389+312	2.73+2.50	14.47+14.71	20.24+29.22	32.25+28.00	14.93+16.85	3823+5164	30.59+10.23
2005	11189496+29887484	17.66+9.31	27.26+17.40	27.26+17.40	27.26+17.40	2014+1224	36.95+9.23	20.19+8.21	9.87+3.09	9.45+3.14	7.41+17.53	2228+3457	1.68+6.23	1.23+3.07	10.17+18.84	51.47+29.53	29.20+21.69	8128+3626	40.42+15.41
2006	9699612+13964939	48.40+19.03	12.76+6.88	12.76+6.88	12.76+6.88	2056+833	37.29+5.22	21.63+9.70	10.45+5.11	10.16+3.85	3.93+2.22	5556+5490	1.85+2.92	11.83+24.40	21.16+32.24	25.73+33.54	39.42+38.65	17160+17780	32.21+16.86
2007	1785459+3114341	40.05+17.03	17.76+9.12	17.76+9.12	17.76+9.12	1616+872	44.72+6.53	15.35+5.17	14.61+5.75	9.64+2.63	0.53+0.44	1851+2104	4.27+10.39	20.57+23.73	6.26+8.67	9.57+13.36	53.61+28.29	9600+11757	33.00+20.06

Romero et al.

noflagellate cysts			Planktonic Foraminifera				Pteropods			
Upwelling relaxation	Potential toxic	Cosmopolitan	Flux	Upwelling	Cool waters	Warm waters	Flux	Uncoiled	L. bulimoides	H. inflatus
Relative abundance (%)			(shells m^{-2} d^{-1})	Relative abundance (%)			(shells m^{-2} d^{-1})	Relative abundance (%)		
5.46+8.48	1.61+1.55	56.38+8.26	2286+2801	22.76+20.69	63.77+26.21	2.29+3.30	326+741	1.18+4.85	0.00+0.00	65.88+44.88
0.73+0.62	4.92+8.90	52.04+14.46	1228+1129	19.00+13.57	49.42+28.58	17.53+24.59	221+838	1.56+6.25	4.38+17.50	86.88+33.01
1.26+1.57	0.83+1.07	63.85+15.69	1287+1417	20.87+23.64	28.54+25.30	31.83+30.75	1962+2342	10.25+8.66	31.00+29.23	43.50+30.83
2.12+2.07	4.13+9.75	57.33+18.81	996+1373	22.32+20.49	52.20+21.22	7.01+8.18	1034+1981	10.49+14.48	15.61+32.41	64.63+36.75

Table 4: Average daily fluxes diatoms (valves m^{-2} d^{-1}), coccolithophores (coccoliths m^{-2} d^{-1}), calcareous and organic dinoflagellate cysts (cysts m^{-2} d^{-1}), planktonic foraminifera and pteropods (shells m^{-2} d^{-1}) and average relative contribution of groups of taxa for each of the above-mentioned microorganisms calculated at site CBeu for full calendar years 2004, 2005, 2006 and 2007.

Table 5   Romero et al.

Diatoms	References
1) Benthic	Round et al. (1990)
Actinoptychus spp.	
Amphora spp.	
Cocconeis spp.	
Cymatosira belgica	
Delphineis surirella	
Grammatophora marina	
Licmophora sp.	
Odontella mobiliensis	
Psammodyction panduriformis	
Tabullaria spp.	
2) Coastal upwelling	Hasle and Syvertsen (1996)
Resting spores of:	
Chaetoceros affinis	
Chaetoceros cinctus	
Chaetoceros compresus	
Chaetoceros constrictus	
Chaetoceros coronatus	
Chaetoceros debilis	
Chaetoceros diadema	
Chaetoceros radicans	
3) Coastal planktonic	Crosta et al. (2012), Romero et al. (2009, 2012, 2016, 2017),
Actinocyclus curvatulus	
Actinocyclus octonarius	
Actinocyclus subtilis	
Chaetoceros concavicornis (vegetative cell,	
Chaetoceros lorenzianus (VC)	
Chaetoceros pseudobrevis (VC)	
Coscinosdiscus argus	
Coscinosdiscus decrescens	
Coscinosdiscus radiatus	
Cyclotella litoralis	
Skeletonema costatum	
Thalassionema nitzschioides var. *capitulata*	
Thalassiosira angulata	
Thalassiosira conferta	
Thalassiosira oestrupii var. *venrickae*	
Thalassiosira poro-irregulata	
4) Open-ocean	Hasle and Syvertsen (1996), Romero et al. (2005), Crosta et al. (2012)
Asteromphalus flabellatus	
Asteromphalus sarcophagus	
Azpetia neocrenulata	
Azpetia nodulifera	
Azpetia tabularis	
Detonula pumila	
Dytilum brightwellii	
Fragilariopsis doliolus	
Hemiaulus hauckii	
Hemidiscus membranaceus	
Leptocyclindrus mediterraneus	
Neodelphineis denticula	
Nitzschia bicapitata	
Nitzschia capuluspalae	
Nitzschia interruptestriata	
Nitzschia sicula	
Planktoniella sol	
Pseudo-nitzschia inflata var. *capitata*	
Pseudo-nitzschia pungens	
Pseudo-nitzschia subfraudulenta	
Pseudosolenia calcar-avis	
Pseudotriceratium punctatum	
Rhizosolenia acuminata	
Rhizosolenia bergonii	
Rhizosolenia imbricatae	
Rhizosolenia setigera	
Roperia tessellata	
Stellarima stellaris	
Thalassionema bacillare	
Thalassionema frauenfeldii	
Thalassionema nitzschioides var. *capitulata*	
Thalassionema nitzschioides var. *inflata*	
Thalassionema nitzschioides var. *parva*	
Thalassiosira eccentrica	
Thalassionema endoseriata	
Thalassiosira ferelineata	
Thalassiosira lineata	
Thalassiosira nanolineata	
Thalassiosira oestrupii var. *oestrupii*	
Thalassiosira sacketii var. *sacketii*	
Thalassiosira sacketii var. *plana*	
Thalassiosira subtilis	
Thalassiosira symmetrica	

Coccolithophores	
1) Cosmopolitan	Boeckel and Baumann (2008), Baumann and Boeckel (2013), Poulton et al. (2017) Young et al. (2019)
Emiliania huxleyi	
Gephyrocapsa oceanica	
2) Lower photic zone	
Algirosphaera robusta	
Calciosolenia murrayi	
Florisphaera profunda	
Gladiolithus flabellatus	
Hayaster perplexus	
3) Warm oligotrophic surface waters	
Discosphaera tubifera	
Helicosphaera carteri	
Rhabdosphaera xiphos	
Umbellosphaera irregularis	
Umbellosphaera tenuis	
Umbilicosphaera anulus	
Umbilicosphaera sibogae	

4) Other miscellanous species
Acanthoica quattrospina
Calcidiscus leptoporus
Calcidiscus leptoporus small
Calcidiscus quadriperforatus
Gephyrocapsa ericsonii
Gephyrocapsa muellerae
Ophiaster hydroideus
Ophiaster hydroideus
Rhabdosphaera stylifer
Syracosphaera anthos
Syracosphaera pulchra

Calcareous dinoflagellates cysts

1) Upwelling — Siggelkow et al. (2002); Richter et al. (2007); Kohn and Zonneveld (2010)
Calciodinellum operosum
Scrippsiella trochoidea
2) Warm waters
Calciodinellum albatrosianum
3) Mineral input
Leonella granifera
4) Cosmopolitan
Thoracosphaera heimii
5) Others
Calciodinellum levantinum
Melodemuncula berlinensis
Pernambugia tuberosa
Scrippsiella lacrymosa
Scrippsiella regalis
Scrippsiella trifida

Organic dinoflagellates cysts

1) Upwelling — Susek et al. (2005); Holzwarth et al. (2010); Trainer et al. (2010); Smayda (2010); Smayda and Trainer (2010); Zonneveld et al. (2010; 2013)
Echinidinium aculeatum
Echinidinium granulatum
Echinidinium transparantum
Echinidinium zonneveldiae
Echinidinium spp.
cyst of *Protoperidinium americanum*
cyst of *Protoperidinium monospinum*
Stelladinium stellatum
2) Upwelling relaxation
Lingulodinium machaerophorum
cyst of *Polykrikos schwartzii*
cyst of *Polykrikos kofoidii*
3) Potential toxic
cysts of *Gymnodinium* spp.
cysts of *Alexandrium* spp.
4) Cosmopolitan
Brigantedinium spp.
Spiniferites species
Impagidinium species

Planktonic Foraminifera

1) Warmer waters — Hemleben et al. (1989), Schiebel and Hemleben (2017)
Globigerinoides ruber (pink and white)
Globigerinoides sacculifer
2) Cooler waters
Globorotalia inflata
Neogloboquadrina incompta
3) Upwelling
Globigerina bulloides
4) Additional secondary species
Beella digitata (Brady 1879)
Globigerinella calida (Parker 1962)
Globigerinella siphonifera (d'Orbigny 1839)
Globorotalia crassaformis (Galloway and Wissler 1927)
Globorotalia menardii (Parker, Jones and Brady 1865)
Globorotalia scitula (Brady 1882)
Globorotalia truncatulinoides (d'Orbigny 1839)
Neogloboquadrina dutertrei (d'orbigny 1839)
Orbulina universa (d'Orbigny 1839)
Pulleniatina obliquiloculata (Parker and Jones 1865)

Pteropods

Heliconoides inflatus (d'Orbigny 1835, formerly known as *Limacina inflata*) — WoRMS Editorial Board (2017)
Limacina bulimoides (d'Orbigny 1835)

1318

Table 5: Species composition of the assemblage of (a) diatoms, (b) coccolithophores, (c)
calcareous and (d) organic dinoflagellate cysts, (e) planktonic foraminifera and (f) pteropods at
site CBeu between June 2003 and March 2008.

1320